A protease and a lipoprotein jointly modulate the conserved ExoR-ExoS-ChvI signaling pathway critical in *Sinorhizobium meliloti* for symbiosis with legume hosts

Julian A. Bustamante [1¶], Josue S. Ceron [1¶], Ivan Thomas Gao [1¶], Hector A. Ramirez [1¶], Milo V. Aviles [1], Demsin Bet Adam [1], Jason R. Brice [1], Rodrigo Cuellar [1], Eva Dockery [1], Miguel Karlo Jabagat [1], Donna Grace Karp [1], Joseph Kin-On Lau [1], Suling Li [1], Raymondo Lopez-Magaña [1], Rebecca R. Moore [1], Bethany Kristi R. Morin [1], Juliana Nzongo [1], Yasha Rezaeihaghighi [1], Joseph Sapienza-Martinez [1], Tuyet Thi Kim Tran [1], Zhenzhong Huang [1], Aaron J. Duthoy [2], Melanie J. Barnett [2], Sharon Long [2], and Joseph C. Chen [1*]

[1] Department of Biology, San Francisco State University, San Francisco, California, United States of America

[2] Department of Biology, Stanford University, Stanford, California, United States of America

* Corresponding author

E-mail: chenj@sfsu.edu (JCC)

¶ Julian A. Bustamante, Josue S. Ceron, Ivan Thomas Gao, Hector A. Ramirez contributed equally to this work. Author order was determined alphabetically.

Running title: proteolytic regulation of ExoR

Abstract word count: 221

Abstract

Sinorhizobium meliloti is a model alpha-proteobacterium for investigating microbe-host interactions, in particular nitrogen-fixing rhizobium-legume symbioses. Successful infection requires complex coordination between compatible host and endosymbiont, including bacterial production of succinoglycan, also known as exopolysaccharide-I (EPS-I). In *S. meliloti* EPS-I production is controlled by the conserved ExoS-ChvI two-component system. Periplasmic ExoR associates with the ExoS histidine kinase and negatively regulates ChvI-dependent expression of *exo* genes, necessary for EPS-I synthesis. We show that two extracytoplasmic proteins, LppA (a lipoprotein) and JspA (a metalloprotease), jointly influence EPS-I synthesis by modulating the ExoR-ExoS-ChvI pathway and expression of genes in the ChvI regulon. Deletions of *jspA* and *lppA* led to lower EPS-I production and competitive disadvantage during host colonization, for both *S. meliloti* with *Medicago sativa* and *S. medicae* with *M. truncatula*. Overexpression of *jspA* reduced steady-state levels of ExoR, suggesting that the JspA protease participates in ExoR degradation. This reduction in ExoR levels is dependent on LppA and can be replicated with ExoR, JspA, and LppA expressed exogenously in *Caulobacter crescentus* and *Escherichia coli*. Akin to signaling pathways that sense extracytoplasmic stress in other bacteria, JspA and LppA may monitor periplasmic conditions during interaction with the plant host to adjust accordingly expression of genes that contribute to efficient symbiosis. The molecular mechanisms underlying host colonization in our model system may have parallels in related alpha-proteobacteria.

Author summary

Symbiotic bacteria that live in the roots of legume plants produce biologically accessible nitrogen compounds, offering a more sustainable and environmentally sound alternative to industrial fertilizers generated from fossil fuels. Understanding the multitude of factors that contribute to successful interaction between such bacteria and their plant hosts can help refine strategies for improving agricultural output. In addition, because disease-causing microbes share many genes with these beneficial bacteria, unraveling the cellular mechanisms that facilitate host invasion can reveal ways to prevent and treat infectious diseases. In this report we show that two genes in the model bacterium *Sinorhizobium meliloti* contribute to effective symbiosis by helping the cells adapt to living in host plants. This finding furthers knowledge about genetics factors that regulate interactions between microbes and their hosts.

Introduction

Rhizobia-legume symbioses account for a substantial proportion of terrestrial nitrogen fixation, converting molecular dinitrogen to a reduced, more bioavailable form such as ammonia (Herridge *et al.*, 2008). Optimization of such biological nitrogen fixation in agriculture may reduce reliance on industrial fertilizers and their negative environmental impacts, including fossil fuel consumption, release of greenhouse gas, and eutrophication (Ferguson *et al.*, 2010; Graham & Vance, 2003; Olivares *et al.*, 2013). The mutualistic relationship requires complex communication and coordination between specific rhizobia and compatible legume plants (Long, 2016; Masson-Boivin & Sachs, 2018), as well as bacterial adaptation to the “stresses” of the host plant environment (Hawkins & Oresnik, 2021; Ledermann *et al.*, 2021). Flavonoids released by the host plant induce bacterial production of essential signaling molecules called Nod factors, lipochitooligosaccharides that elicit root hair curling, plant cell division, and nodule development (Gibson *et al.*, 2008). Colonization of nodules typically begins with bacterial cells invading the root hair via plant cell wall-derived tunnels called infection threads, followed by release into the nodule primordium and engulfment into symbiosomes, membrane-bound organelles in the plant cytoplasm, in which the rhizobia differentiate into bacteroids capable of fixing nitrogen in exchange for carbon compounds from the host (Barnett & Fisher, 2006; Poole *et al.*, 2018). The root nodules can be determinate or indeterminate, depending on the host: one major distinction is that determinate nodules lack a persistent meristem and contain cells at similar stages of development, whereas indeterminate nodules exhibit a sequential gradient of development, with dividing cells in the meristem at one end, next to progressive zones of invasion, nitrogen fixation, and senescence (Ferguson *et al.*, 2010).

The alphaproteobacterium *Sinorhizobium meliloti* and its compatible hosts, including *Medicago sativa* (alfalfa) and *M. truncatula* (barrel medic), emerged as models for indeterminate nodulation (Jones *et al.*, 2007). Alfalfa is a major feed crop, its annual production valued at over $11 billion in the U.S. alone (USDA Crop Values 2022 Summary), while *M. truncatula* serves as a genetically tractable reference species (Burks *et al.*, 2018). Factors found to be critical for *S. meliloti* to form mutualistic symbiosis have been shown to play similar roles during host infection in related pathogens, such as *Brucella* spp., suggesting mechanistic parallels between mutualism and pathogenesis (Jones *et al.*, 2007). One such shared mechanism is the ExoS-ChvI two-component phosphorelay pathway, conserved across related alpha-proteobacteria,

particularly within the Rhizobiales group (Greenwich *et al.*, 2023; Heavner *et al.*, 2015). ExoS is a membrane-bound histidine kinase with a periplasmic sensor domain, while ChvI is its cognate response regulator (Cheng & Walker, 1998b). Mutations in ExoS and ChvI as well as their orthologs in other endosymbionts, including BvrS-BvrR in the mammalian pathogen *Brucella abortus* and ChvG-ChvI in the plant pathogen *Agrobacterium tumefaciens*, impair host colonization (Alakavuklar *et al.*, 2023; Bélanger *et al.*, 2009; Charles & Nester, 1993; Chen *et al.*, 2008; Mantis & Winans, 1993; Sola-Landa *et al.*, 1998; Vanderlinde & Yost, 2012; Wang *et al.*, 2010a; Wells *et al.*, 2007). A third component of the signaling system, ExoR, acts as a periplasmic repressor of ExoS via physical association (Chen *et al.*, 2008; Wells *et al.*, 2007). ExoR is regulated by proteolysis (Lu *et al.*, 2012; Wiech *et al.*, 2015; Wu *et al.*, 2012), and binding to ExoS protects it from degradation (Chen *et al.*, 2008). Mutations in *S. meliloti* ExoR also disrupt symbiosis (Chen *et al.*, 2008; Doherty *et al.*, 1988; Ozga *et al.*, 1994; Wells *et al.*, 2007; Yao *et al.*, 2004), but the ExoR ortholog in *B. abortus* seems dispensable for virulence (Castillo-Zeledón *et al.*, 2021), and mutation in *A. tumefaciens exoR* interferes with binding to plant root surfaces while permitting disease progression (Tomlinson *et al.*, 2010). These observations may reflect a more nuanced role of ExoR during host invasion.

Cues that suggest transition into the host environment appear to stimulate the ExoR-ExoS-ChvI signaling cascade to promote a developmental shift from free-living to symbiotic (Greenwich *et al.*, 2023). Acidic pH that mimics the rhizosphere leads to degradation of ExoR and induction of the ChvG-ChvI pathway in *A. tumefaciens* (Heckel *et al.*, 2014; Li *et al.*, 2002; Wu *et al.*, 2012; Yuan *et al.*, 2008). In *B. abortus*, a combination of acidic pH and nutrient limitation, conditions similar to those found during passage through autophagosome-like compartments, activates BvrS-BvrR signaling (Altamirano-Silva *et al.*, 2021; Altamirano-Silva *et al.*, 2018; Rivas-Solano *et al.*, 2022). However, conditions that specifically trigger the ExoR-ExoS-ChvI pathway in *S. meliloti* remain elusive (Bélanger *et al.*, 2009; Keating, 2007; Ratib *et al.*, 2018), and different cues for divergent species are possible. Furthermore, some cues may directly activate the ExoS sensor kinase and bypass ExoR: recent studies indicate that peptidoglycan stress induces the *A. tumefaciens* ChvG-ChvI system independently of ExoR (Williams *et al.*, 2022), and that in *S. meliloti*, membrane disruption due to a phosphatidylcholine deficiency activates ExoS without a concomitant decrease in steady-state levels of ExoR (Geiger *et al.*, 2021). In the free-living alphaproteobacterium *Caulobacter crescentus*, which lacks an ExoR ortholog, the ChvG-ChvI system was shown to be stimulated by various stresses, including DNA damage, acidic pH,

126 osmotic upshift, and inhibition of cell wall synthesis (Frohlich *et al.*, 2018; Quintero-Yanes *et al.*,
127 2022; Stein *et al.*, 2021).
128
129 Irrespective of the specific triggers, the ExoR-ExoS-ChvI system influences a multitude of
130 physiological activities, including exopolysaccharide (EPS) production, motility, biofilm
131 formation, cell envelope maintenance, and nutrient utilization, befitting its pivotal regulation of
132 symbiotic development (Bélanger *et al.*, 2009; Wang *et al.*, 2010a; Wells *et al.*, 2007; Yao *et al.*,
133 2004). Similarly, orthologs in *A. tumefaciens* and *Bartonella henselae* control parallel processes
134 crucial for pathogenesis (Alakavuklar *et al.*, 2021; Heckel *et al.*, 2014; Quebatte *et al.*, 2010). In
135 *B. abortus*, BvrS and BvrR also coordinate diverse functions and upon activation directly target
136 genes involved in metabolite deployment, cell envelope modulation, cell division, and virulence
137 (Guzman-Verri *et al.*, 2002; Lamontagne *et al.*, 2007; Manterola *et al.*, 2007; Manterola *et al.*,
138 2005; Martinez-Nunez *et al.*, 2010; Rivas-Solano *et al.*, 2022; Viadas *et al.*, 2010). Initial
139 transcriptome profiles of *S. meliloti exoS*::Tn*5* and *exoR*::Tn*5* mutants revealed altered
140 expression of hundreds of genes (Wells *et al.*, 2007; Yao *et al.*, 2004), but subsequent
141 interrogation that included identification of genomic regions bound by ChvI winnowed the direct
142 targets of the response regulator down to 64, many known to participate in physiological
143 activities described above (Chen *et al.*, 2009; Ratib *et al.*, 2018). Perhaps illustrating the
144 complex interaction of regulatory pathways and the difficulty of signal deconvolution, a
145 significant fraction of ChvI targets also changed expression with other published perturbations
146 (Ratib *et al.*, 2018), including acid stress (de Lucena *et al.*, 2010; Draghi *et al.*, 2016; Hellweg *et*
147 *al.*, 2009), antimicrobial peptide treatment (Penterman *et al.*, 2014), phosphate starvation (Krol
148 & Becker, 2004), cyclic nucleotide accumulation (Krol *et al.*, 2016), overexpression of SyrA
149 (Barnett & Long, 2015), and mutations in *podJ*, *cbrA*, *ntrY*, and *emrR* (Calatrava-Morales *et al.*,
150 2017; Fields *et al.*, 2012; Gibson *et al.*, 2007; Santos *et al.*, 2014).
151
152 One key subset of the regulon induced upon ExoS-ChvI activation is the *exo* genes, responsible
153 for synthesis of succinoglycan, or EPS-I, originally characterized in *S. meliloti* strain Rm1021 as
154 the only symbiotically active EPS (Becker *et al.*, 2002; Long *et al.*, 1988; Pellock *et al.*, 2000;
155 Reuber & Walker, 1993). An increase in EPS-I production, usually concomitant with a decrease
156 in flagellar motility (Alakavuklar *et al.*, 2021; Ratib *et al.*, 2018), represents a physiological
157 transition from saprophytic to endosymbiotic, as EPS-I contributes to successful interaction
158 between compatible symbiotic partners. Mutants that lack EPS-I or synthesize variants with
159 altered structures (for example, absence of succinylation) exhibit defects in the initiation or

elongation of infection threads, while changes in EPS-I levels can influence symbiotic efficiency (Barnett & Long, 2018; Cheng & Walker, 1998a; Geddes *et al.*, 2014; Jones, 2012; Mendis *et al.*, 2016); thus, both the quality and quantity of EPS-I matter during infection. EPS-I may serve as a recognition signal, particularly for suppressing host defenses (Jones *et al.*, 2008). When *Mesorhizobium loti* invades *Lotus japonicus*, a legume host that develops determinate nodules, recognition of bacterial EPS by a plant receptor-like kinase facilitates symbiosis, as mutants that do not produce EPS can still form symbiosis, whereas those that synthesize inappropriate, truncated forms of EPS cannot, and the plant receptor is required to restrain infection by bacteria with inappropriate EPS (Kawaharada *et al.*, 2015; Kawaharada *et al.*, 2017; Kelly *et al.*, 2013). While no corresponding plant receptor for *S. meliloti* EPS-I has been identified so far (Maillet *et al.*, 2020), EPS-I does enhance tolerance of various environmental assaults (Miller-Williams *et al.*, 2006; Vriezen *et al.*, 2007), including those encountered during host colonization, such as acidity, oxidative stress, and antimicrobial peptides (Arnold *et al.*, 2018; Arnold *et al.*, 2017; Davies & Walker, 2007; Hawkins *et al.*, 2017; Lehman & Long, 2013).

In particular, EPS-I confers resistance to the antimicrobial activity of NCR247 (Arnold *et al.*, 2018; Arnold *et al.*, 2017), which belongs to a diverse family of small, nodule-specific cysteine-rich (NCR) peptides encoded by legumes in the inverted-repeat-lacking clade (IRLC), where plants with indeterminate nodules typically reside (Mergaert *et al.*, 2003; Poole *et al.*, 2018; Van de Velde *et al.*, 2010). Structurally similar to characterized defensins (Maroti *et al.*, 2015), different NCR peptides regulate bacterial load *in planta* and influence distinct aspects of terminal bacteroid differentiation, including maintaining survival and preventing premature senescence (Cao *et al.*, 2017; Farkas *et al.*, 2014; Horváth *et al.*, 2015; Kim *et al.*, 2015; Sankari *et al.*, 2022; Wang *et al.*, 2010b). In addition to EPS-I, other bacterial factors can modulate the effects of NCR peptides (Arnold *et al.*, 2017; Benedict *et al.*, 2021). For example, BacA, long recognized as critical in both *S. meliloti* and *B. abortus* for host colonization (LeVier *et al.*, 2000), reduces membrane permeabilization and cell death induced by NCR247 *ex planta* (Haag *et al.*, 2011). Some *S. meliloti* strains produce HrrP, a peptidase capable of degrading NCR peptides, attenuating their antimicrobial effects and altering the host ranges of the bacteria (Price *et al.*, 2015). These molecular arsenals for exerting control evoke the Red Queen hypothesis, which proposes that coevolving partners engage in a continual arms race to maintain the relationship (Brockhurst, 2011; Van Valen, 1973): “it takes all the running you can do, to keep in the same place” (Carroll, 1900 [1872]).

One of the genes previously identified in a transposon-based screen as necessary for *S. meliloti* resistance against NCR247 *ex planta* is SMc03872, which encodes a periplasmic protease conserved in alpha-proteobacteria and confers a competitive advantage during symbiosis with alfalfa (Arnold *et al.*, 2017). SMc03872 was also identified in a genetic selection for suppressors that ameliorated the osmosensitivity of a *podJ* null mutant (Fields *et al.*, 2012). That work demonstrated that PodJ is a conserved polarity factor that contributes to cell envelope integrity and EPS-I production in *S. meliloti*, and that deletion of SMc03872 or SMc00067, encoding a lipoprotein, reduced EPS-I levels. Here we show that SMc03872 and SMc00067 jointly influence EPS-I production by lowering the steady-state levels of periplasmic ExoR and thus activating the ExoS-ChvI signal transduction pathway. This regulation contributes to competitive fitness during host colonization, suggesting that SMc03872 and SMc00067 facilitate transition to a gene expression pattern more suitable for the host environment.

Results

LppA and JspA jointly contribute to EPS-I biosynthesis and symbiotic competitiveness

In a previous suppressor analysis to identify mutants that alleviated the cell envelope defects of the *podJ1* deletion strain, we found two genes (SMc00067 and SMc03872) whose interruption or deletion led to consistent and significant reduction in EPS-I production (Fields *et al.*, 2012). SMc00067 (annotated as *lppA*) encodes a 148-amino acid lipoprotein, while SMc03872 (here named *jspA*, for *podJ* suppressor protease A) encodes a 497-amino acid metalloprotease that contains an M48 peptidase domain, with a conserved HEXXH active site, and a LysM domain, commonly associated with peptidoglycan binding (Fig. 1) (Arnold *et al.*, 2017; Becker *et al.*, 2009; Galibert *et al.*, 2001). BLAST searches against representative bacterial species indicated that both genes are highly conserved within the Rhizobiales group of alphaproteobacteria, based on shared synteny and protein sequences (Boratyn *et al.*, 2013). Outside of the Rhizobiales group, orthologs of LppA were rare or difficult to identify, while the sequence similarities of JspA homologs were generally lower than those found within Rhizobiales (Table S1). Both LppA and JspA contain lipoprotein signal peptides at their N-termini, each with a stretch of hydrophobic amino acids followed by an invariant Cys within the lipobox motif (Fig. 1B) (Juncker *et al.*, 2003). In the original annotation for LppA, the protein starts seven codons upstream of the LAGC lipobox, with VVASGVA, but N-terminal extension of 12 codons adds more hydrophobic amino acids, allowing a more optimal signal sequence; thus, we have numbered the amino acid sequence accordingly. The lipoprotein signals suggest that each protein is exported out of the cytoplasm and attached to the inner or outer membrane (Kovacs-Simon *et al.*, 2011).

To verify that LppA and JspA contribute to EPS-I production, we performed complementation analysis by introducing plasmids carrying *lppA* or *jspA* under the control of a taurine-inducible promoter (P_{tau}) (Mostafavi *et al.*, 2014) into wild-type or deletion strains. Serial dilutions of strains were spotted onto plates containing calcofluor, which fluoresces when bound to EPS-I (Finan *et al.*, 1985). Consistent with previously published results (Fields *et al.*, 2012), *lppA* or *jspA* deletion strain carrying the empty vector exhibited lower levels of EPS-I production, with 60-70% of calcofluor fluorescence compared to wild-type strains carrying the vector, in the absence or presence of taurine (Fig. 2A and 2B). Wild-type and deletion strains with plasmids carrying *lppA* or *jspA* showed similar fluorescence levels as their counterparts with the vector in

the absence of taurine and elevated fluorescence levels in the presence of taurine. Similar results were obtained with the closely related *S. medicae* strain WSM419: deletion of the *lppA* or *jspA* ortholog in that strain reduced fluorescence on plates containing calcofluor (Fig. S1A), and complementation with the heterologous *S. meliloti* gene rescued the defect (Fig. S1B, strains JOE5290 and JOE5264). At higher taurine concentrations (5 and 10 mM), induction of *jspA* expression in *S. meliloti* Rm1021 inhibited colony formation (Fig. 2C), but this effect was not observed with *lppA* expression, even with the highest possible concentration of taurine (100 mM) (Fig. 2A). While induction of *lppA* or *jspA* expression promoted EPS-I production in wild type or corresponding deletion strains, *lppA* expression in the *jspA* mutant (Fig. 2A, bottom image) and *jspA* expression in the *lppA* mutant (Fig. 2B, bottom image) failed to increase calcofluor fluorescence. Furthermore, *jspA* overexpression did not cause growth arrest in the *lppA* mutant (Fig. 2D). These results suggest that LppA and JspA act in concert to stimulate EPS-I production.

Since EPS-I is critical for infection thread formation during host colonization, we asked if deletion of *lppA* or *jspA* leads to a symbiosis defect. *M. sativa* seedlings were inoculated with wild-type Rm1021 or Δ*lppA* or Δ*jspA* derivatives, and *M. truncatula* seedlings were inoculated with wild-type WSM419 or its Δ*lppA* or Δ*jspA* derivatives because WSM419 forms more efficient symbiosis with *M. truncatula* than *S. meliloti* strains (Ghosh *et al.*, 2021; Larrainzar *et al.*, 2014; Terpolilli *et al.*, 2008). We did not observe obvious differences in plant growth and the development of root nodules on nitrogen-free medium over the course of four weeks: the average numbers of pink, nitrogen-fixing nodules per plant were similar 21 and 28 days after inoculation with different bacterial strains (Table S2), suggesting that the two genes are not required for symbiosis. To examine more closely if LppA and JspA contribute to efficient host colonization, we conducted competitive infection assays in which seedlings were inoculated with mixtures containing equal numbers of two strains, and bacteria were recovered from root nodules 28 days post-inoculation to determine occupancy rates (Materials and methods). One or both strains were marked with distinct antibiotic resistance to facilitate identification via plating after extraction from nodules. *M. sativa* plants were inoculated with mixtures of Rm1021 derivatives (Fig. 3A), while *M. truncatula* plants were inoculated with mixtures of WSM419 derivatives (Fig. 3B). Consistent with previous reports (Fields *et al.*, 2012; Gage, 2002), we found that a small percentage of the nodules contained mixed populations of bacteria, while the majority of nodules were dominated by one strain. Discounting those nodules containing mixed populations, roughly equal numbers of nodules (45 – 55%) were occupied by each strain when

the inoculum contained two wild-type strains (marked or unmarked). In contrast, *lppA* or *jspA* mutants were recovered from significantly fewer nodules (6 – 26% of the nodules) when competed against wild-type strains (Fig. 3 and Table S3). These results align with previous demonstration that JspA is important for protection against the NCR247 antimicrobial peptide and for competitiveness during symbiosis between *S. meliloti* and *M. sativa* (Arnold *et al.*, 2017). Furthermore, our results show that both JspA and LppA contribute to competitiveness, in two different model symbiotic interactions.

JspA and LppA affect expression of EPS-I and flagellar genes

Next, we investigated how JspA and LppA may influence EPS-I production by determining if they affect gene expression in *S. meliloti*. First, we used a transcriptional fusion to the β-glucuronidase (GUS) reporter gene (Chen *et al.*, 2009) to measure expression of *exoY*, encoding a galactosyltransferase required for EPS-I biosynthesis (Reuber & Walker, 1993). Expression levels were examined in both PYE and LB rich media because our past experiences indicated that differences between strains could be more apparent in one particular medium (Fields *et al.*, 2012). Consistent with EPS-I levels monitored via calcofluor fluorescence (Fig. 2), deletion of *jspA* or *lppA* reduced *exoY* expression to 55 - 72% of wild-type levels, in both LB and PYE media (Table 1). Second, we examined reporter fusions to *flaC* and *mcpU* (Gibson *et al.*, 2007), respectively encoding a flagellin and a chemoreceptor (Hoang *et al.*, 2008; Scharf & Schmitt, 2002), as expression of genes involved in flagellar motility and chemotaxis often change in opposition to those involved in EPS-I production (Bahlawane *et al.*, 2008; Barnett *et al.*, 2004; Fields *et al.*, 2012). Deletion of *jspA* or *lppA* increased expression of these two genes significantly in LB medium (to 134 - 159% of wild type), but less clearly in PYE medium (to 114 - 129% of wild type) (Table 1). Finally, expression levels of *exoY*, *flaC*, and *mcpU* in the Δ*jspA* Δ*lppA* double mutant were similar to those in the single mutants (Table 1), again suggesting that JspA and LppA function in the same genetic pathway.

We also used the transcriptional fusions to *exoY* and *flaC* to assess the effects of constitutive *jspA* or *lppA* expression from a plasmid-borne, taurine-inducible promoter (with the same P_{tau}-regulated constructs as those in Fig. 2) (Table 2). Induction of *jspA* expression with 10 mM taurine in PYE for three hours was sufficient to significantly alter expression of both *exoY* and *flaC* in the wild-type background. Such induction also complemented the drop in *exoY* expression seen in the Δ*jspA* mutant. In contrast, induction of *lppA* expression did not affect *flaC* or *exoY* significantly under various conditions tested (Table 2). We only found a modest

311 increase in *exoY* transcription in the wild-type background when *lppA* expression was induced
312 for six hours with 100 mM taurine in LB medium. Such induction also sufficed to complement
313 the drop in *exoY* expression in the Δ*lppA* mutant. Notably, overexpression of *jspA* could not
314 reverse the decrease in *exoY* expression in the Δ*lppA* mutant, and overexpression of *lppA* could
315 not reverse the same effect in the Δ*jspA* mutant. Overall, expression analysis with
316 transcriptional reporters reflected the results obtained with calcofluor fluorescence (Fig. 2): *lppA*
317 appears to require higher concentrations of the taurine inducer compared to *jspA* to cause
318 detectable physiological changes, and both genes need each other to function.
319
320 To determine if LppA acts as a lipoprotein and JspA acts as a protease, we mutated the lipobox
321 motif of LppA and the peptidase domain of JspA (Fig. 1B) and assessed the mutant derivatives'
322 effects on EPS-I synthesis and gene expression. For LppA, we mutated Cys_{23} of the lipobox
323 motif to Ser and tagged both the wild-type and mutant versions at the C-terminus with an HA
324 epitope. While constructing the *lppA-HA* allele, we serendipitously obtained alleles with
325 conversion of Gly_{96} to Trp and Ala_{78} to Ser and decided to analyze each of the corresponding
326 two mutants as well. Due to the relatively minor changes in reporter gene expression when
327 *lppA* was overexpressed in the wild-type background (Table 2), we mainly examined the
328 functionality of various *lppA* alleles in the Δ*lppA* background. Overexpression of these various
329 derivatives ($LppA_{C23S}$, LppA-HA, $LppA_{C23S}$-HA, $LppA_{G96W}$-HA, $LppA_{A78S}$-HA) in the Δ*lppA* mutant
330 from the plasmid-borne P_{tau} promoter did not increase the fluorescence levels of colonies on
331 calcofluor plates compared to the vector-only control, whereas overexpression of LppA did (Fig.
332 4A). Induction of LppA or LppA-HA significantly elevated expression of the *exoY* fusion reporter
333 to similar levels (180 – 195% of that in the Δ*lppA* mutant with the vector), while $LppA_{C23S}$ and
334 $LppA_{C23S}$-HA did not (Table 3). The other two variants, $LppA_{G96W}$-HA and $LppA_{A78S}$-HA,
335 increased *exoY* expression modestly but significantly (123 – 130%) (Table 3). Immunoblot
336 analysis using antibodies against the HA epitope indicated that the steady-state levels of all HA-
337 tagged derivatives of LppA, when constitutively expressed from plasmids, are relatively similar
338 in wild-type, Δ*lppA*, and Δ*jspA* backgrounds, except for $LppA_{C23S}$-HA, which appears to be
339 expressed at very low levels in all backgrounds (Fig. 4B). These results suggest that acylation
340 at the lipobox Cys allows LppA to anchor to the membrane and mature into a stable lipoprotein.
341 Addition of an HA epitope at the C-terminus appears to reduce the functionality of LppA, while
342 the G96W and A78S mutations further diminish protein activity without affecting its stability
343 detectably.
344

For JspA, we mutated residues within the HEMAH active site, His147 to Ala, or Glu148 to Ala or Asp (Fujimura-Kamada *et al.*, 1997), and tagged wild-type and mutant versions at the C-terminus with the HA epitope. When constitutively expressed from the plasmid-borne P_{tau} promoter in the wild-type background with 5 mM taurine, both JspA and JspA-HA elevated the fluorescence of colonies on calcofluor plates, but only JspA inhibited colony formation (Fig. 4C). None of the three active site mutants (H147A, E148A, E148D), untagged or tagged, enhanced fluorescence or affected growth. In addition, we expressed *S. meliloti* JspA and its derivatives in three related alphaproteobacteria -- *S. medicae* WSM419, *S. fredii* NGR234, and *C. crescentus* NA1000 -- to assess if JspA activity is conserved (Fig. S1B, S2). In WSM419, expression of JspA complemented the EPS-I production defect of the Δ*jspA* mutant, whereas expression of $JspA_{E148A}$ did not (Fig. S1B). In both WSM419 and NGR234, overexpression of JspA inhibited colony formation, while overexpression of $JspA_{E148A}$-HA did not (Fig. S2). Overexpression of $JspA_{E148A}$ and JspA-HA inhibited growth to different extents in these two species (Fig. S2), suggesting that JspA variants have different activities in distinct genetic backgrounds: overproduction of a proteolytically inactive JspA seems more deleterious in NGR234 than in *S. meliloti* Rm1021 or *S. medicae* WSM419. In contrast, expression of JspA and its derivatives in the more distantly related NA1000 did not inhibit growth until higher levels of induction (10 mM taurine), possibly due to the general stress of protein overproduction because similar levels of inhibition were observed for all alleles.

Results similar to those seen with calcofluor plates were obtained when analyzing JspA derivatives with transcriptional fusion of the GUS reporter to *exoY* in *S. meliloti*: overexpression of JspA-HA significantly increased *exoY* transcription, but to a lesser extent compared to untagged JspA (Table 3). As with JspA, JspA-HA also increased *exoY* expression in the Δ*jspA* mutant but not in the Δ*lppA* mutant, again indicating that JspA needs LppA for activity. The E148A and E148D variants, untagged or tagged, both failed to elevate *exoY* expression to levels achieved by JspA and JspA-HA, indicating that the active site of the protease is necessary for function. Immunoblotting indicated that HA-tagged versions of JspA appear to reach similar steady-state levels in wild-type, Δ*lppA*, and Δ*jspA* backgrounds (Fig. 4D, 4E), demonstrating that variations in activity are not likely due to differences in protein stability in different genetic backgrounds. Together, these results suggest that the active site of JspA is critical for its proteolytic activity, but other domains contribute to function and may interfere with cellular processes when overexpressed, consistent with previous demonstration by Arnold *et al.*

(2017) that the peptidase active site, the lipobox motif, and the LysM domain are all necessary for protection against the antimicrobial activity of NCR247.

LppA and JspA participate in the ExoR-ExoS-ChvI signaling pathway

Considering that LppA and JspA are likely extracytoplasmic, we wondered how they influence transcription of EPS-I and flagellar genes. To uncover their mechanism of action, we performed whole-genome expression analysis using Affymetrix GeneChips (Barnett *et al.*, 2004). Having generated mutant alleles and determined growth conditions and strain backgrounds with which significant changes in gene expression could be observed, we decided to examine the transcriptomes of Rm1021 carrying an empty vector or overexpressing wild-type JspA or loss-of-function $JspA_{E148A}$ from a plasmid. As expected, overexpression of JspA caused changes in a substantial set of genes, whereas $JspA_{E148A}$ did not: pairwise comparisons for changes greater than 1.5-fold revealed 198 genes with significantly different expression between strains overexpressing JspA and carrying the vector, 155 genes between JspA and $JspA_{E148A}$, and only 5 genes between $JspA_{E148A}$ and the vector (Fig. 5A, Table S4). 141 gene expression changes were shared between the JspA versus vector and JspA versus $JspA_{E148A}$ comparisons, and consequently these genes were deemed strong candidates for the JspA transcriptome: 80 increased expression and 61 decreased expression during JspA overexpression. Consistent with measurements of *exoY* and *flaC* reporter fusions (Tables 2 and 3), a sizable portion of up-regulated genes are associated with exopolysaccharide biosynthesis, while the majority of down-regulated genes are associated with flagellar motility and chemotaxis. One up-regulated target that stood out is *chvI*, encoding a conserved response regulator critical for viability and symbiosis (Cheng & Walker, 1998b; Ratib *et al.*, 2018). To verify the results of the transcriptome analysis, we constructed transcriptional fusions of the GUS reporter to *chvI* and select candidates of the JspA transcriptome. Measurements of GUS activity showed expected increase (for SMc01580, *pckA*, and *chvI*) or decrease (for *mcpU*) when *jspA* expression is induced with taurine from the plasmid-borne P_{tau} promoter, compared to the same wild type carrying the vector; in contrast, overexpression of the mutant $jspA_{E148A}$ allele did not elicit significant changes (Table 4). We also evaluated expression of the *chvI* reporter when JspA and variants were expressed from a plasmid-borne, IPTG-inducible promoter, P_{lac} (Khan *et al.*, 2008) to ensure that the observed changes could be replicated with another inducer. Overexpression of JspA and JspA-HA both increased *chvI* transcription, whereas $JspA_{E148A}$, untagged or tagged, did not cause similar effects (Table 4). These reporter activities support the validity of the transcriptome analysis.

412

413 Knowing that the ExoR-ExoS-ChvI signaling system can control its own expression (Lu &
414 Cheng, 2010; Ratib *et al.*, 2018), we asked if JspA participates in that regulatory pathway. We
415 compared the JspA transcriptome against the published transcriptomes of ExoR/ExoS and ChvI
416 (Chen *et al.*, 2009; Ratib *et al.*, 2018; Wells *et al.*, 2007) (see Materials and methods for details)
417 and saw substantial overlap among the three sets of genes (Fig. 5B). In contrast, the JspA
418 transcriptome had minimal overlap with the published transcriptome of RpoH1, a heat shock
419 sigma factor (Fig. 5C) (Barnett *et al.*, 2012), chosen for comparison because it represented a
420 stress response distinct from that of the ExoR-ExoS-ChvI system. Hypergeometric probability
421 tests (Lund *et al.*, 2002) indicated that overlap among the JspA, ExoR/ExoS, and ChvI
422 transcriptomes are highly significant, whereas each of the three sets overlapped poorly with the
423 RpoH1 transcriptome (Table S5). As noted previously (Ratib *et al.*, 2018), there are significant
424 overlaps between the ChvI regulon and the groups of genes affected by the *podJ1* mutation
425 (Fields *et al.*, 2012) or by NCR247-treatment (Penterman *et al.*, 2014). To be expected for one
426 sharing the same genetic pathway as ChvI, JspA's transcriptome also intersects significantly
427 with the *podJ1* and NCR247 sets (Table S6). These similarities suggest that JspA contributes
428 to a regulatory pathway, likely the ExoR-ExoS-ChvI system, for responding to specific stress
429 conditions, such as those caused by the *podJ1* mutation or exposure to NCR247.
430
431 To determine if JspA and LppA influence the ExoR-ExoS-ChvI signaling pathway, we conducted
432 epistasis analysis, first using Tn*5* insertions in *exoR* and *exoS* that lead to overproduction of
433 EPS-I (Doherty *et al.*, 1988). Strains carrying the *exoS96*::Tn*5* insertion produce an N-
434 terminally truncated ExoS that behaves like a constitutively active kinase (Cheng & Walker,
435 1998b), while strains carrying the *exoR95*::Tn*5* insertion produce a C-terminally altered ExoR
436 that has lost function (Lu *et al.*, 2012). Loss of *lppA* or *jspA* in these backgrounds did not
437 reduce EPS-I synthesis, suggesting that *exoR* and *exoS* are epistatic to *lppA* and *jspA* (Fig. 6A).
438 Considering that, like ExoR, mature JspA and LppA are predicted to reside in the periplasm,
439 and ExoR inhibits ExoS-ChvI signaling, we hypothesized that JspA and LppA together
440 negatively regulate ExoR activity (Fig. 6B). This model is consistent with JspA and LppA being
441 unable to reduce EPS-I production if ExoR is inoperative or if ExoS is constitutively active. To
442 test this idea further, we constructed a ChvI depletion strain, in which the only copy of *chvI* is
443 under the control of P_{lac} on a pBBR1-derived plasmid (Khan *et al.*, 2008). As ChvI is essential
444 for growth on rich medium, the ChvI depletion strain grew poorly in the absence of the IPTG
445 inducer and normally in its presence, similar to a *chvI*$^{+}$ strain carrying the same plasmid grown

in the absence or presence of IPTG (Fig. S3). We then monitored expression of the *exoY* reporter when ChvI is replete or depleted and when wild-type or mutant JspA is overexpressed from the P_{tau} promoter on a compatible RK2-derived plasmid (Mostafavi *et al.*, 2014) (Fig. 6C). In a *chvI*$^{+}$ strain carrying the P_{lac} vector or the P_{lac}-*chvI* plasmid, constitutive expression of JspA from P_{tau} increased *exoY* expression compared to the same strain carrying the P_{tau} vector (Fig. 6C, first four strains on the left), consistent with previous measurements (Tables 2 and 3). In the ChvI depletion strain carrying the P_{tau} vector, shutting off *chvI* expression by removing IPTG for six hours reduced *exoY* expression (Fig. 6C, fifth strain from left). When JspA was overexpressed in the ChvI depletion strain, *exoY* expression was high when ChvI was replete in the presence of IPTG (Fig. 6C, sixth strain from left, + IPTG), comparable to that seen in *chvI*$^{+}$ strains when JspA was overexpressed. However, depletion of ChvI in the absence of IPTG prevented *exoY* expression from becoming elevated by JspA (Fig. 6C, sixth strain from left, - IPTG). A ChvI depletion strain overexpressing $JspA_{E148A}$ (Fig. 6C, rightmost strain) yielded similar *exoY* expression patterns as the depletion strain carrying the P_{tau} vector (Fig. 6C, fifth strain from left). These results support the model that JspA functions upstream of ChvI: increasing JspA levels relieves the inhibitory activity of ExoR, in turn activating the ExoS sensor kinase and ChvI response regulator and promoting expression of EPS-I genes and thus EPS-I production. In the absence of ChvI, JspA is unable to stimulate expression of EPS-I genes, such as *exoY*.

The rhizobial ExoR-ExoS-ChvI system effects changes in gene expression in response to environmental conditions, including acid stress (Altamirano-Silva *et al.*, 2018; Heckel *et al.*, 2014; Yuan *et al.*, 2008). Since JspA and LppA appear to act upstream of the system, we investigated if they mediate transmission of environmental signals. We compared the JspA transcriptome and ChvI regulon against sets of genes that changed expression upon acid stress, identified in three different studies (de Lucena *et al.*, 2010; Draghi *et al.*, 2016; Hellweg *et al.*, 2009). Hypergeometric probability tests indicate that the overlaps between the JspA transcriptome or ChvI regulon and each of the three sets of acid response genes are significant but not as strong as that between JspA and ChvI: the most significant overlaps with the JspA transcriptome and ChvI regulon belong to the set identified by Hellweg, Pühler, and Weidner (2009) (Table S7). However, the overlaps between the JspA transcriptome or ChvI regulon with each of the three sets of acid response genes are comparable to, if not better than, overlaps among the three. Thus, we chose four representative genes (SMb21188, SMc01580, *exoY*, and *chvI*) from the JspA transcriptome and ChvI regulon that also appeared in one or more of

the acid responses and examined their expression via reporter fusions in acidic, neutral, or basic pH. All four reporter fusions increased expression when wild-type Rm1021 was grown at pH 6 compared to pH 7; only *exoY* showed significant increase at pH 8.5 as well (Fig. 7). Deletion of *jspA* or *lppA* appeared to curtail this increase in response to acid stress, more obviously for SMb21188 and SMc01580 (Fig. 7A and 7B, pink bars). For *exoY* and *chvI*, the deletions reduced reporter expression compared to wild type at neutral pH (Fig. 7C and 7D, yellow bars), and the fold-change between pH 6 and pH 7 in the deletion strains approximated that seen in wild type (Fig. 7C and 7D, red percentages). Nevertheless, in the deletion mutants, the increase in *exoY* expression due to growth at pH 6 was impacted more severely than the increase due to growth at pH 8.5 (Fig. 7C). Our results suggest that, while factors other than ChvI may help regulate *exoY* and *chvI* expression upon acid stress, JspA and LppA facilitate ChvI's response to acid stress.

JspA and LppA enhance ExoR degradation

Because JspA is predicted to be a periplasmic protease, and JspA and LppA appear to promote ExoS/ChvI activity, in opposition to ExoR, which can be regulated via proteolysis (Lu *et al.*, 2012; Wu *et al.*, 2012), we assessed whether JspA reduces ExoR levels. We introduced a plasmid expressing *jspA* or *jspA*$_{E148A}$ from P$_{lac}$ into a strain with *exoR-V5* allele instead of *exoR* at the native locus. Induction of *jspA* expression with 1 mM IPTG in rich media inhibited growth, starting 3 – 4 hours after induction (Fig. 8A and Fig. S4). Overexpression of *jspA*$_{E148A}$ did not retard growth compared to a strain carrying the P$_{lac}$ vector when cultures were grown in flasks (Fig. S4B and S4C) but did modestly slow growth in 48-well plates (Fig. 8A and S4A). We monitored steady-state levels of ExoR-V5 by immunoblotting with antibodies against the V5 epitope, at 0, 3, and 6 hours after induction. ExoR-V5 level was detectably lower in the strain overexpressing JspA compared to strains carrying the vector or expressing mutant JspA$_{E148A}$, six hours after induction (Fig. 8B). Our transcriptomic analysis indicated that *exoR* expression is slightly elevated (1.3x) (Table S4) when *jspA* is constitutively induced. This increase in *exoR* expression was verified using transcriptional fusion to the GUS reporter (Fig. 8C). Thus, the decrease in ExoR level is not attributable to a drop in *exoR* expression. Instead, JspA appears to negatively regulate ExoR at the protein level. The reduction in ExoR likely stimulates the ExoS-ChvI pathway, resulting in feedback that elevates *exoR* transcription, as previously described (Lu & Cheng, 2010).

To eliminate changes in ExoR levels due to transcriptional regulation, we placed a FLAG-tagged version of *exoR* under the control of the P_{lac} promoter on a plasmid and induced expression with 0.5 mM IPTG in rich medium. Immunoblotting with anti-FLAG antibodies revealed a band for the mature ExoR-FLAG protein at ~29 kDa, as well as a band with slightly larger molecular mass, indicative of the pre-processed form (computed to be 32 kDa with the signal peptide) (Fig. 9A, lane 2). We also observed additional bands with smaller molecular masses, likely representing degradation products (Lu *et al.*, 2012). In the *jspA*$^+$ background, overexpression of JspA-HA reduced the steady-state level of ExoR-FLAG, compared to when the strain carried the vector or expressed mutant $JspA_{E148A}$-HA (Fig. 9A, lanes 2 – 4; 9B). In the Δ*jspA* background, ExoR-FLAG levels were elevated compared to wild type, and overexpression of JspA-HA reduced that elevation, while $JspA_{E148A}$-HA did not (Fig. 9A, lanes 6 – 8). Probing with antibodies against the HA epitope indicated that steady-state levels of JspA-HA and $JspA_{E148A}$-HA were comparable. Expression of untagged versions of JspA and JspAE148A in both the Δ*jspA* and *jspA*$^+$ backgrounds (Fig. 9A, lanes 10 – 13) led to similar effects as the corresponding HA-tagged variants on ExoR-FLAG, indicating that the tagged and untagged versions of JspA behaved similarly in this assay. Next, we examined steady-state levels of ExoR-FLAG when LppA is present or absent. Again, overexpression of JspA-HA reduced ExoR-FLAG levels in both *jspA*$^+$ and Δ*jspA* strains (Fig. 9B, lanes 1 and 3), compared to the same strains expressing mutant $JspA_{E148A}$-HA (Fig. 9B, lanes 2 and 4). However, in the Δ*lppA* background, overexpression of JspA-HA did not reduce ExoR-FLAG levels compared to overexpression of $JspA_{E148A}$-HA (Fig. 9B, lanes 5 and 6). These results reinforce that JspA and LppA concertedly regulate the ExoR-ExoS-ChvI pathway by reducing ExoR protein levels.

To demonstrate further that JspA and LppA participate in ExoR proteolysis, we expressed the three proteins in two heterologous systems, *C. crescentus* NA1000 and *E. coli* DH10B, both of which lack clear *lppA* and *exoR* orthologs and contain weak *jspA* orthologs (Table S1). In NA1000, ExoR-FLAG was expressed from a P_{lac} promoter on a pBBR1-based plasmid, while different combinations of JspA variants and LppA were co-transcriptionally expressed from a P_{tau} promoter on a compatible RK2-derived plasmid. When ExoR-FLAG was expressed in the absence of JspA or LppA, we detected both the mature and pre-processed forms of the protein, as well as various degradation products, by immunoblotting with anti-FLAG antibodies (Fig. 10A, lane 2). Expression of JspA, but not mutant $JspA_{E148A}$, reduced the steady-state level of mature ExoR-FLAG but did not affect the pre-processed form (Fig. 10A, lanes 3 and 4). Levels of mature ExoR-FLAG dropped further when LppA was expressed along with JspA or JspA-HA

(Fig. 10A, lanes 5 and 7); this reduction did not happen when LppA was expressed with untagged or tagged versions of $JspA_{E148A}$ (Fig. 10A, lanes 6 and 8). Intriguingly, one of the ExoR-FLAG degradation products, approximately 20-kDa in size, became more prominent when only JspA, untagged or HA-tagged, was expressed (Fig. 10A, lane 3; Fig. S5A, lanes 5 and 9), but lost this prominence when LppA was co-expressed with JspA (Fig. 10A, lanes 5 and 7; Fig. S5A, lanes 7 and 11). Similar results were observed in *E. coli* DH10B, in which ExoR-FLAG was again expressed from the same P_{lac} promoter on a pBBR1-based plasmid, while expression of wild-type or mutant JspA-HA and varying levels of LppA-HA was achieved by placing different constructs under the control of a weakened P_{trc} promoter on a pBR322-based plasmid (Weiss *et al.*, 1999) (see Materials and methods) (Fig. S5B, File S1). In DH10B, expression of JspA-HA alone did not reduce the steady-state level of ExoR-FLAG (lane 2 in both Fig. 10B and S5B, lane 2), but co-expression of JspA-HA and LppA-HA did (lanes 4 and 6 in both Fig. 10B and S5B). Furthermore, the extent of reduction in ExoR-FLAG levels depended on the level of LppA-HA expression, such that mature ExoR-FLAG became undetectable when LppA-HA was highly overexpressed (Fig. S5B, lane 8). This decrease in ExoR-FLAG levels failed to occur in the presence of mutant $JspA_{E148A}$-HA (for example, lane 7 in both Fig. 10B and S5B). These degradation patterns in *C. crescentus* and *E. coli* suggest that LppA assists JspA to proteolyze ExoR.

Discussion

In this report, we demonstrated that two lipoproteins, JspA and LppA, jointly contribute to the production of EPS-I by regulating expression of relevant biosynthesis genes. Each also contributes to competitiveness in nodule colonization during symbiosis with *Medicago* hosts. Site-directed mutagenesis indicated that the lipobox motif of LppA and active site residues of the JspA protease are critical for their functions, consistent with annotations of predicted domains. Transcriptome, epistasis, and Western blot analyses further revealed that the two lipoproteins influence signaling through the conserved ExoS-ChvI two-component pathway and modulate the steady-state levels of ExoR, a periplasmic inhibitor of ExoS. Exposure to acidic pH is a potential cue for activating the signaling pathway.

These results suggest a model in which JspA and LppA, in response to cell envelope stress such as acid shock, facilitate the degradation of ExoR, thus enhancing phosphorelay in the ExoS-ChvI system, which generates physiological changes to counter the stress (Fig. 6B). This regulation via proteolysis appears analogous to how *E. coli* and other Gram-negative bacteria respond to envelope stress with the Cpx and sigma(E) pathways (Mitchell & Silhavy, 2019; Raivio, 2005). For the Cpx response, accumulation of misfolded proteins in the periplasm can cause DegP to degrade CpxP, a periplasmic inhibitor of the CpxAR two-component system (Isaac *et al.*, 2005). For the sigma(E) response, unfolded outer membrane proteins activate a proteolytic cascade involving DegS and RseP to degrade RseA, an inner membrane anti-sigma factor that inhibits sigma(E) (Alba *et al.*, 2002; Walsh *et al.*, 2003). While the exact molecular signal that induces degradation of ExoR is unknown, our results (Fig. 7) and evidence from other rhizobia (Altamirano-Silva *et al.*, 2018; Heckel *et al.*, 2014) indicate that acidic pH can activate the ExoS-ChvI pathway, possibly by causing protein misfolding in the cell envelope. Most likely, various other cell envelope perturbations can also potentiate the signal: for example, cell wall stress resulting from inhibition of the essential penicillin-binding protein PBP1a has recently been shown to activate the ExoS-ChvI pathway (Williams *et al.*, 2022), and JspA's LysM domain, predicted to bind peptidoglycans, was shown to be critical for protection against the antimicrobial peptide NCR247 (Arnold *et al.*, 2017). This model can accommodate a number of scenarios for how JspA and LppA jointly respond to envelope stress: for instance, LppA may enable the proper folding or positioning of JspA in the membrane, or misfolding of LppA may directly induce JspA's proteolytic activity. In particular, the complex physical

properties of the outer membrane (Cao & Wall, 2020; Sun *et al.*, 2022) necessitate multiple regulatory checkpoints, and LppA may sense its integrity, analogous to the *E. coli* RcsF lipoprotein (Tata *et al.*, 2021), and transmit disturbances to JspA. Alternatively, LppA may monitor or participate in the crosslink between the outer membrane and the cell wall (Godessart *et al.*, 2021), and disruptions in the process are relayed to JspA. Other envelope proteins that influence ExoS-ChvI signaling, such as SyrA (Barnett & Long, 2015), may also participate in the activation. Further investigation to elucidate the precise mechanisms involved would advance understanding of stress response in rhizobia.

Notably, the *jspA* and *lppA* genes were originally identified in a suppressor analysis of a *podJ1* mutant, which exhibits pleiotropic defects in the cell envelope (Fields *et al.*, 2012): while the *podJ1* mutant grew poorly on LB medium with low salt concentrations, null mutations in *jspA* or *lppA* alleviated the growth defect. A subdued envelope stress response when JspA or LppA is absent may allow better growth of the *podJ1* mutant under specific conditions, as too much activation can be deleterious. This interpretation is consistent with the suggestion that stress response requires careful management to avoid toxicity (Mitchell & Silhavy, 2019). For example, deletion of *rseA* in *E. coli* causes constitutive activation of the sigma(E) system, resulting in membrane defects associated with lethality in stationary phase (Nicoloff *et al.*, 2017). Similarly, loss of *exoR* in *S. meliloti* led to lethality, or at least severely thwarted growth (Arnold *et al.*, 2017; diCenzo *et al.*, 2018; Flores-Tinoco *et al.*, 2020; Price *et al.*, 2018), just as overexpression of *jspA* did in the present study, presumably due to hyperactivation of the ExoS-ChvI pathway. Deletion of *exoR* does not appear to retard growth as strongly in related rhizobia such as *B. abortus* and *A. tumefaciens* (Castillo-Zeledón *et al.*, 2021; Heckel *et al.*, 2014), consistent with ExoS and ChvI being critical for growth in *S. meliloti* (Bélanger *et al.*, 2009; Wang *et al.*, 2010a) but not in these two other genetic models (Charles & Nester, 1993; Sola-Landa *et al.*, 1998). Whether *exoR*, *exoS*, and *chvI* orthologs are required for viability appears to vary in other rhizobia as well (Baraquet *et al.*, 2021; Lai *et al.*, 2016; Perry *et al.*, 2016). This variability in the impact of conserved signaling pathways is not unprecedented. For example, sigma(E) is essential in *E. coli* (De Las Peñas *et al.*, 1997) but not in *S. typhimurium* (Humphreys *et al.*, 1999; Testerman *et al.*, 2002).

Effective management of envelope perturbations allows adaptation to environmental changes, including those encountered during symbiosis (from mutualistic to pathogenic) (Hawkins & Oresnik, 2021; Hews *et al.*, 2019). As impairment of ExoS and ChvI disrupts symbiosis (Barnett

& Long, 2015; Bélanger *et al.*, 2009; Wang *et al.*, 2010a; Wells *et al.*, 2007; Yao *et al.*, 2004), and their orthologs are required for virulence in *A. tumefaciens* and *B. abortus* (Charles & Nester, 1993; Sola-Landa *et al.*, 1998), *S. meliloti* likely modulates ExoS-ChvI signaling to promote gene expression patterns conducive to invasion and persistence within a eukaryotic host (Ratib *et al.*, 2018; Wells *et al.*, 2007), akin to pathogenic Gram-negative bacteria that use the Cpx and sigma(E) pathways to express virulence factors to ensure survival during infection (Fang *et al.*, 2016; Hews *et al.*, 2019; Raivio, 2005; Taylor *et al.*, 2014). For instance, JspA and LppA may contribute to competitiveness by ensuring an appropriate degree of EPS-I production, as the level of symbiotic EPS can optimize interaction with plant hosts (Jones, 2012). Other genes regulated by JspA probably also contribute to efficient symbiosis. For example, JspA inhibits expression of the transcription regulator LdtR, which plays a role in osmotic stress tolerance, motility, and likely cell wall remodeling (Barnett *et al.*, 2019; Pagliai *et al.*, 2014). JspA increases expression of *lsrB*, which encodes a LysR-family transcription factor required for effective nodulation (Luo *et al.*, 2005) and involved in the differential expression of over 200 genes, including many that regulate redox homeostasis (An *et al.*, 2021). Deletion of *lsrB* resulted in poor growth and increased sensitivity to the detergent deoxycholate (Barnett *et al.*, 2019), and *lsrB* orthologs in *B. abortus* and *A. tumefaciens* contribute to pathogenesis (Budnick *et al.*, 2020; Eisfeld *et al.*, 2021; Sheehan *et al.*, 2015; Tang *et al.*, 2018). In addition, a significant fraction of the JspA transcriptome consists of genes of unknown function, and changes in their expression may promote fitness during host colonization as well. Many uncharacterized genes in the ExoS-ChvI regulon, and by extension the JspA transcriptome, are predicted to be translocated out of the cytoplasm and envelope-associated, making them more likely to interact with the host environment and to maintain barrier integrity (Ratib *et al.*, 2018). In particular, *jspA* was shown to confer resistance to the nodule-specific antimicrobial peptide NCR247 (Arnold *et al.*, 2017). One possible explanation is that JspA changes gene expression patterns via ExoS-ChvI to counter such host defenses. Nevertheless, other possible explanations, not mutually exclusive, can also account for JspA's involvement in resistance against cell envelope assaults: for example, JspA may degrade other substrates or signaling pathways under specific conditions, or JspA and LppA may assist in the proper construction of the cell envelope by ensuring proper maturation of other lipoproteins. Furthermore, a number of other signaling systems, such as ActK-ActJ, CenK-CenR, CpxA-CpxR, EmmB-EmmC, FeuQ-FeuP, and NtrX-NtrY, contribute to the maintenance of cell envelope integrity in rhizobia (Albicoro *et al.*, 2021; Albicoro *et al.*, 2023; Barnett & Long, 2018; Bensig *et al.*, 2022; Calatrava-Morales *et al.*, 2017; Griffitts *et al.*, 2008; Lakey *et al.*, 2022; Morris & Gonzalez,

669 2009; Santos *et al.*, 2010; VanYperen *et al.*, 2015; Wang *et al.*, 2013; Xing *et al.*, 2022), and
670 how these different systems cooperate with ExoS-ChvI to ensure successful symbiosis remains
671 ripe for further investigation.
672
673
674

Materials and methods

Bacterial strains, growth conditions, and genetic manipulations

Strains derived from *Sinorhizobium meliloti* Rm1021 (Meade *et al.*, 1982) and *S. medicae* WSM419 (Reeve *et al.*, 2010) used for this study are listed in Table S8. Other alphaproteobacterial strains used were *S. fredii* NGR234 (Stanley & Cervantes, 1991; Trinick, 1980) and *C. crescentus* NA1000 (Evinger & Agabian, 1977). *E. coli* strains DH5α and DH10B strains (both from Invitrogen) were used for molecular cloning, gene expression, and maintenance of plasmids, which are listed in Table S9. *Sinorhizobium* strains were cultured at 30°C in LB, TY, or PYE media; *C. crescentus* was cultured at 30°C in PYE; and *E. coli* strains were cultured at 30 or 37°C in LB (Fields *et al.*, 2012). When appropriate, antibiotics, agar, sucrose, and/or calcofluor were added at previously published concentrations (Barnett *et al.*, 2000; Fields *et al.*, 2012). IPTG and taurine were added as inducers (Mostafavi *et al.*, 2014) at concentrations described in the text. For pH shifts, LB medium was buffered with 20 mM 2-(*N*-morpholino)ethanesulfonic acid (MES), 3-(*N*-morpholino)propanesulfonic acid (MOPS), or Tris, and adjusted to pH 6, 7, or 8.5, respectively, with HCl or NaOH. Growth of cultures was monitored by measuring absorbance at 600 nm (A_{600}), with aliquots from tubes or flasks or with a BioTek Synergy H1m plate reader if grown in 48-well plates. Mobilization of plasmids from *E. coli* to *Sinorhizobium* or *Caulobacter* strains via triparental mating, N3-mediated generalized transduction, and two-step allelic replacement by homologous recombination were all performed as previously described (Fields *et al.*, 2012; Finan *et al.*, 1986; Griffitts & Long, 2008; House *et al.*, 2004; Martin & Long, 1984; Quandt & Hynes, 1993). Standard techniques were used for manipulation and analysis of DNA, including PCR amplification, restriction digests, agarose gel electrophoresis, ligation, and transformation (Ausubel *et al.*, 1998; Sambrook *et al.*, 1989). Plasmids and DNA fragments were purified using commercial kits (Qiagen). Elim Biopharmaceuticals synthesized custom oligonucleotides and provided Sanger DNA sequencing services.

Expression in *E. coli*

ExoR-FLAG was expressed in *E. coli* from an IPTG-inducible P_{lac} promoter on pMB859, derived from the pSRKKm vector (Khan *et al.*, 2008). To co-express JspA-HA, $JspA_{E148A}$-HA, and LppA-HA, we constructed plasmids derived from pDSW204, which is compatible with pSRKKm and also allows IPTG induction with a weakened P_{trc} promoter (Weiss *et al.*, 1999): pJC720,

pJC730, pJC731, pJC733, pJC734, pJC735, pJC736, and pJC737 (Fig. S5, File S1). Plasmids pJC720 and pJC733 carry wild-type *jspA-HA* and mutant *jspA*$_{E148A}$*-HA*, respectively, including 18 nucleotides upstream of *jspA*'s annotated start codon. We added *lppA-HA* to these plasmids in three different configurations and assessed their expression empirically. For pJC730 and pJC735, the ribosome binding site (RBS) of *E. coli araB* (Guzman *et al.*, 1995) was appended upstream of *lppA-HA* and inserted after *jspA-HA* or *jspA*$_{E148A}$*-HA*. For pJC731 and pJC736, *lppA-HA*, along with 54 nucleotides upstream of its originally annotated start codon (18 nucleotides upstream of the new start codon suggested in this report), was inserted after wild-type or mutant *jspA-HA*. For pJC734 and pJC737, *lppA-HA* and its upstream sequence were inserted in front of wild-type or mutant *jspA-HA*. We intended the RBS of *araB* to enhance expression of *lppA-HA* in *E. coli*, but that configuration (pJC730 and pJC735) yielded the lowest levels of expression (Fig. 10). Because *lppA-HA* is in-frame with wild-type or mutant *jspA-HA* on pJC731, pJC734, pJC736, and pJC737, read-through translation (Ryoji *et al.*, 1983) appeared to produce low levels of fusion proteins that were sometimes detectable on Western blots (Fig. 10 and S5).

Homology and domain analysis

Orthologs in representative genomes and their sequence similarities to the query were determined via BLAST (Boratyn *et al.*, 2013). Genomic contexts are presented as annotated in the National Center for Biotechnology Information (NCBI) database (Sayers *et al.*, 2022). Protein domains were predicted using InterPro (Blum *et al.*, 2021), Pfam (Mistry *et al.*, 2021), and LipoP (Juncker *et al.*, 2003).

Calcofluor assays

EPS-I production was assess as previously described (Fields *et al.*, 2012), with LB plates containing 0.02% calcofluor white M2R (MP Biomedicals). Liquid cultures were calibrated to the same optical density (A_{600} of 0.2 – 0.5) and serially diluted ten-fold in water, and four or five µL of the 10^{-2} to 10^{-6} dilutions were each spotted onto calcofluor plates containing appropriate additives, such as taurine for induction and oxytetracycline for plasmid selection. Dilutions were at times spotted onto PYE plates as well for comparison. Plates were examined and photographed after 3-4 days of incubation with a Kodak 4000MM Pro Image Station, with its associated Carestream MI software and filters (430 nm excitation and 535 nm emission). The fluorescence intensity of each spot was standardized relative to the corresponding wild-type

control on the same plate, and the average values of the 10^{-2} to 10^{-4} spots from at least three independent plates were compared.

β-glucuronidase (GUS) assays

Transcriptional fusions for β-glucuronidase (GUS) assays were constructed, and GUS activities in different strains under various growth conditions were determined, as previously described (Fields *et al.*, 2012; Swanson *et al.*, 1993). Fusions to *uidA* were introduced into the genome using nonreplicating plasmids, and the wild-type function of the corresponding gene was preserved (Table S9, File S1). Cells were lysed after measuring the optical density of the culture (A_{600}), and PNPG (*p*-nitrophenyl-β-D-glucuronide) was incubated with the lysed cells until the mixture turned light yellow, when A_{415} was measured. GUS activity was derived according to the formula: A_{415} x 1000 / [(incubation time in minutes) x (culture volume in mL) x A_{600}]. *p* values and statistical significance were determined using t-test (two-tailed, unequal variance).

Symbiosis assays

Symbiotic association between *Sinorhizobium* strains and *Medicago* plants was assessed as previously described (Fields *et al.*, 2012; Griffitts *et al.*, 2008; Li, 2018; Oke & Long, 1999). Alfalfa (*M. sativa* GT13Rplus) and barrel medic (*M. truncatula* cultivar Jemalong A17) were cultivated individually in 18x150-mm glass tubes on agar slants made with standard nodulation medium [as described in (Crook *et al.*, 2012), except with 2 mM KH_2PO_4 and 0.5 mM MES, pH 6.3] and 11.5 g/L Phyto agar (PlantMedia); seeds were surface-sterilized with 70% ethanol and 50% bleach, rinsed with water, germinated in inverted 100x25-mm Petri dishes, placed on agar slants, and allowed to grow for three days at 22°C under fluorescent lamps (16-h day length) before inoculation. *M. sativa* was inoculated with *S. meliloti* Rm1021 strains, while *M. truncatula* was inoculated with *S. medicae* WSM419 strains because WSM419 is a better symbiotic partner for *M. truncatula* compared to *S. meliloti* strains, including Rm1021 (Ghosh *et al.*, 2021; Larrainzar *et al.*, 2014; Terpolilli *et al.*, 2008). Bacterial cells grown to mid-logarithmic phase were suspended in water to an A_{600} of 0.1, and each seedling was inoculated with 0.1 mL of the suspension [approximately 10^7 colony-forming units (CFU)]. The numbers of white and pink nodules that developed on plant roots were recorded at 14, 21, and 28 days post inoculation (dpi). Initially white nodules turn pink due to production of leghemoglobin, indicative of nitrogen fixation (Jones *et al.*, 2007). For competitive colonization assays, equal volumes of two cell suspensions (with A_{600} of 0.1) were mixed and then diluted ten-fold, and each seedling was

inoculated with 0.1 mL of the diluted mixture (approximately 10^6 CFU). (For three of the 12 competitive assays with WSM419 strains, trials D1, D3, and E1, the inoculating mixtures were not diluted, and each seedling received 10^7 CFU). The CFU and ratios of strains in the inoculating mixtures were determined by plating serial dilutions on PYE containing streptomycin, nalidixic acid, neomycin, or spectinomycin. Symbiosis competitiveness was assessed 28 dpi by harvesting nodules, surface-sterilizing them individually with 10% bleach, crushing each in PYE medium, and plating serial dilutions of the extracts: 10 µL each of 10^{-1} to 10^{-4} dilutions were dripped to form lines on plates, and colonies were counted after three to four days of incubation at 30°C. A nodule was considered to be dominated by a particular strain if more than 80% of the CFU from the extract can be attributed to that strain. Consistent with previous reports (Fields *et al.*, 2012; Gage, 2002), the majority of nodules were dominated by a single strain (Fig. 3, Table S3). For some nodules not dominated by a single strain, colonies recovered on permissive plates (containing streptomycin for Rm1021 and its derivatives, or nalidixic acid for WSM419 and its derivatives) were re-streaked to verify the ratios of strains (Table S3, "patch" columns). In those cases, the nodule was assigned as mixed occupancy if neither strain gave rise to at least 90% of the colonies tested. In some instances, two or more adjacent nodules were harvested together and crushed in the same tube. If such a sample was dominated by a single strain, then it counted as a single nodule for that strain. On the other hand, if the sample yielded a mixture of two strains, then it was excluded from the final tally of that particular competition trial [Table S3, "Mixed (Multi. Nodules)"]. In Fig. 3, *p*-values were calculated using the Mann-Whitney-Wilcoxon test (two-tailed) for the *M. sativa* competitions and the t-test (two-tailed, unequal variances) for the *M. truncatula* competitions. The Mann-Whitney-Wilcoxon test is nonparametric but has less power for smaller sample sizes (and is ineffective for a total sample size less than eight) (Motulsky, 2023); thus, the t-test was more suitable for analyzing the *M. truncatula* competitions, which had fewer trials per category compared to the *M. sativa* competitions. Table S3 provides the t-test *p*-values for competitions in both host plants.

Transcriptome analysis

Microarray analysis of RNA transcripts using custom Affymetrix GeneChips was conducted as previously described (Barnett & Long, 2015; Barnett *et al.*, 2004). RNA purification, cDNA preparation, chip hybridization, fluidics, scanning, and data analysis were performed accordingly (Barnett *et al.*, 2004). Strains JOE3200 (carrying pCM130 vector), JOE4140 (expressing wild-type *jspA*), and JOE4400 (expressing mutant $jspA_{E148A}$) were grown in PYE supplemented with 0.5 µg/mL oxytetracycline and 10 mM taurine for 4.5 hours to mid-logarithmic phase, when cells

were harvested for RNA extraction. Three biological replicates were used for each strain analyzed. Nine pairwise comparisons were made between two strains: a change in signal was considered significant if $p \leq 0.05$. As with other gene array platforms, our DNA chip measures mRNA abundance, which is influenced by both transcription and mRNA decay; we use the term "expression" to include the sum of all factors affecting mRNA abundance. Raw microarray data have been deposited in the NCBI Gene Expression Omnibus (Barrett *et al.*, 2013) under Accession GSE155833. The significance of overlap between transcriptomes or sets of genes was determined using hypergeometric probability test, as previously described (Lund *et al.*, 2002; Ratib *et al.*, 2018). Genes in the ExoR/ExoS transcriptome were deduced from interrogation of *exoR95*::Tn*5* and *exoS96*::Tn*5* mutants that have hyperactive ChvI activity (Wells *et al.*, 2007); thus, many of the changes in gene expression may be indirect or independent of the ExoS-ChvI pathway. In addition, two biological replicates for each strain were used in that experiments (instead of the three used in the current analysis for JspA transcriptome), and that could have contributed to the relatively large number of genes in the ExoR/ExoS transcriptome. The ChvI regulon contains a combination of nonredundant genes from two publications: (1) those that decreased expression in the ChvI(K214T) partial-loss-of-function strain and increased expression in the ChvI(D52E) gain-of-function strain compared to wild type (Chen *et al.*, 2009), and (2) group 1 and group 2 direct targets of ChvI (Ratib *et al.*, 2018).

Western blotting

Immunoblotting was performed using standard procedures (Ausubel *et al.*, 1998; Sambrook *et al.*, 1989): 1.5 mL of culture samples were collected, resuspended in SDS sample buffer (at 150 µL for culture A_{600} of 1), boiled for 5 min, resolved by SDS-PAGE, and transferred to PVDF membrane for detection by chemiluminescence (SuperSignal West Pico). Monoclonal anti-V5 (Invitrogen R960-25; AB_2556564) was used at 1:2500 dilution, anti-HA [clone 2-2.2.14] (Thermo 26183; AB_10978021) used at 1:1000 to 1:5000 dilution, and antibody to *E. coli* ATPase B [7E3F2] (Abcam ab110280) used at 1 ng/mL. Peroxidase-conjugated monoclonal anti-FLAG M2 antibodies (Sigma A8592) were used at 1:2000 to 1:5000 dilution. Peroxidase-conjugated donkey anti-mouse IgG antibodies (715-035-150) were from Jackson ImmunoResearch Lab and used at 1:25,000 dilution. To examine blots containing both HA and FLAG epitopes, we probed the blots first with anti-FLAG antibodies, detected them with chemiluminescent substrates, washed the blots with Tris-buffered saline (Sambrook *et al.*, 1989) containing 0.05% Tween 20 (TBST), then probed with anti-HA primary antibodies and

peroxidase-conjugated secondary antibodies, and imaged again with chemiluminescence. Similarly, to detect both V5 epitope and the beta subunit of ATP synthase, we probed blots first with anti-V5 antibodies, imaged with chemiluminescence, washed the blots with TBST, then probed with antibodies against ATPase B, and treated with chemiluminescence reagents. Images captured in the second detection showed both target epitopes. Each blot image shown is representative of at least two biological replicates.

Data availability

Microarray data have been deposited in the Gene Expression Omnibus (GEO) under accession GSE155833. All plasmid sequences are provided as supporting information (File S1).

Acknowledgements

We thank Esther Chen, Mike Kahn, and Bob Fisher for discussion, support, and carrot cake. Esther Chen also provided critical feedback on the manuscript. We are grateful to past and current laboratory members for their assistance in various aspects of this project, particularly Reyna Benitez, Tanisha Saini, and Noel Lejat for performing GUS assays.

Funding

Research reported in this publication was supported by the National Institute of General Medical Sciences of the National Institutes of Health (NIH) under Award Number SC3-GM096943 to J.C.C. and National Science Foundation (NSF), Division of Integrative Organismal Systems, under Rules of Life Award Number 2015870 to S.R.L. NIH Award Number T34-GM008574 (MARC) provided support for J.A.B., J.S.C., R.C., R.L.-M., and J.N.; R25-GM048972 (Bridge to the Doctorate) supported H.A.R.; R25-GM059298 (MBRS-RISE) supported J.S.-M.; R25-GM050078 (Bridges to the Baccalaureate) supported J.S.C. and R.C.; T34-GM145400 (U-RISE) supported R.C.; and UL1-GM118985, TL4-GM118986, RL5-GM118984 (SF BUILD) supported B.K.R.M. NSF REU DBI Award Number 1156452 provided summer funding for R.L.-M. and R.B., and NSF DBI Award Number 1548297 provided summer funding for H.A.R. R.R.M. was supported by the Beckman Scholars Program. The content is solely the responsibility of the authors and does not necessarily represent the official views of the funding agencies.

Figure legends

FIGURE 1. Schematics of the genomic regions around *lppA* and *jspA* and of their protein products. (A) *S. meilioti lppA* (SMc00067) and *jspA* (SMc03872) share synteny with their respective orthologs in closely related alphaproteobacteria, such as *B. abortus* and *A. tumefaciens*. Gene and ORF names are shown as annotated, with pentagonal arrows indicating directionality. Arrows with the same colors in different species represent probable homologs, with red arrows indicating *lppA* or *jspA* orthologs; genes without annotated functions or obvious orthologs in corresponding regions are depicted with shades of grey. RR and HK signify response regulators and histidine kinases. The drawing is to scale; bar indicates 1 kb. (B) *lppA* encodes a 148-aa lipoprotein, while *jspA* encodes a 497-aa metalloprotease. Both LppA and JspA contain lipoprotein signal peptides at their N-termini; the sequences of these leader peptides are shown, with red arrows indicating cleavage sites before the invariant cysteine of the lipobox motifs, underlined. The N-terminus of LppA was originally annotated as the 13th amino acid (V_{13}) shown here, but extension of 12 amino acids provides a better signal sequence. JspA also contains M48 peptidase and LysM domains; key amino acids of the peptidase domain are displayed. Grey numbers indicate residues that border the predicted protein domains.

FIGURE 2. Calcofluor fluorescence, indicating EPS-I production, of strains expressing *lppA* or *jspA*. Ten-fold serial dilutions (10^{-2} to 10^{-5}) of logarithmic-phase cultures were spotted onto LB plates containing calcofluor and allowed to grow for three days prior to fluorescence imaging. Darker spots on representative images indicate brighter fluorescence. Fluorescence levels were measured relative to the *S. meliloti* Rm1021 wild-type (WT) strain carrying an empty vector on each plate. Averages and standard deviations were calculated from measurements on at least three independent days, with duplicate plates each time. (A) WT, Δ*lppA*, or Δ*jspA* strains carrying the vector (pCM130 or pJC478) or a plasmid with *lppA* under the control of a taurine-inducible promoter (pJC532) were grown on plates containing 0 or 100 mM taurine. (B) WT, Δ*jspA*, or Δ*lppA* strains carrying the vector or a plasmid with *jspA* under the control of a taurine-inducible promoter (pJC535) were grown on plates containing 0 or 2.5 mM taurine. Green bars indicate comparisons when *lppA* is expressed, and those with blue borders indicate comparisons with the Δ*jspA* background. Blue bars indicate comparisons when *jspA* is

914 expressed, and those with green borders indicate comparisons with the Δ*lppA* background. (C)
915 WT or Δ*jspA* strains carrying the vector or expressing *jspA* were grown on plates containing 5 or
916 10 mM taurine. (D) WT or Δ*lppA* strains carrying the vector or expressing *jspA* were grown on
917 plates containing 5 mM taurine. Relative fluorescence was not calculated for 5 or 10 mM
918 taurine due to growth inhibition of select strains.
919
920
921 FIGURE 3. Proportions of root nodules colonized by each bacterial strain after seedlings were
922 inoculated with equal mixtures of two strains. (A) *S. meliloti* Rm1021 and its derivatives were
923 used to infect *M. sativa*, while (B) *S. medicae* WSM419 and its derivatives were used to infect
924 *M. truncatula*. Rm1021 (Ω) is a derivative of Rm1021 marked with resistance to spectinomycin,
925 while WSM419^{R} are derivatives of WSM419 marked with resistance to spectinomycin or
926 neomycin. Mutations in *jspA* or *lppA* in Rm1021 were deletions or transposon insertions, while
927 those in WSM419 were all deletions. Percentages (± standard deviations) below each
928 competition indicate the mean proportions of nodules containing the mutant, wild type (WT), or a
929 mixture of the two, while the graphs depict relative abundance when mixed nodules are
930 excluded. Dark grey circles indicate the percentage of nodules occupied by WT for individual
931 competition trials. Error bars represent standard deviations. *, $p < 0.05$; **, $p < 0.01$. Bottom
932 row of each table [Trials (nodules)] indicates the number of trials (and total number of nodules
933 assessed) per competition. Detailed results from the competitive symbiosis assays are
934 available in Table S3.
935
936
937 FIGURE 4. Expression of mutant *lppA* and *jspA* alleles in *S. meliloti*. (A) Calcofluor
938 fluorescence was used to assess EPS-I production in Δ*lppA* strains expressing different alleles
939 of *lppA* from a taurine-inducible promoter. (B) Immunoblots show steady-state levels of different
940 versions of HA epitope-tagged LppA in wild-type (WT), Δ*lppA*, and Δ*jspA* backgrounds. C23S-
941 HA, G96W-HA, and A78S-HA stand for mutant versions of LppA-HA, encoded by *lppA*$_{C23S}$-*HA*,
942 *lppA*$_{G96W}$-*HA*, and *lppA*$_{A78S}$-*HA*, respectively. Samples were harvested from cultures grown in
943 LB with 100 mM taurine for 6 hours. (C) Wild-type Rm1021 expressing different *jspA* alleles
944 from a taurine-inducible promoter exhibit varying levels of fluorescence on calcofluor plates. (D,
945 E) Immunoblots show steady-state levels of different versions of JspA-HA. E148A-HA, E148D-
946 HA, and H147A-HA stand for mutant versions of JspA-HA, encoded by *jspA*$_{E148A}$-*HA*, *jspA*$_{E148D}$-
947 *HA*, and *jspA*$_{H147A}$-*HA*, respectively. Samples were harvested from (D) wild-type strains grown

948 in LB without or with 10 mM taurine for 3 hours or (E) wild-type, Δ*lppA*, or Δ*jspA* strains grown in
949 PYE with 10 mM taurine for 4.5 hours. Presence or absence of taurine in the growth medium (+
950 or -) or chromosomal *jspA* and *lppA* (+ or Δ) are indicated above each lane. Numbers to the
951 right of immunoblots (B, D) indicate approximate molecular mass standards, in kDa. Plasmids
952 pJC532, pJC605, pJC606, pJC607, pJC608, and pJC609 were used for expressing *lppA*,
953 $lppA_{C23S}$, *lppA-HA*, $lppA_{C23S}$-*HA*, $lppA_{G96W}$-*HA*, and $lppA_{A78S}$-*HA*, while pJC535, pJC555, pJC556,
954 pJC557, pJC558, pJC559, pJC560, pJC561 were used for *jspA*, $jspA_{E148A}$, $jspA_{E148D}$, $jspA_{H147A}$,
955 *jspA-HA*, $jspA_{E148A}$-*HA*, $jspA_{E148D}$-*HA*, and $jspA_{H147A}$-*HA*, respectively. Vectors used were
956 pCM130 (A, D, E) or pJC478 (C). For assessing calcofluor fluorescence (A, C), ten-fold serial
957 dilutions (10^{-2} to 10^{-5}) of logarithmic-phase cultures were spotted onto LB plates without or with
958 taurine, and allowed to grow for three days prior to fluorescence imaging. Darker spots on
959 representative images indicate brighter fluorescence.
960
961
962 FIGURE 5. Venn diagrams depicting overlaps of gene sets. (A) Circles of the Venn diagram
963 represent the numbers of genes whose expression changed >1.5-fold in three pairwise
964 comparisons: between strains that overexpress wild-type JspA or mutant $JspA_{E148A}$ (JspA vs.
965 $JspA_{E148A}$), between strains that overexpress JspA or carry the vector pCM130 (JspA vs.
966 vector), or between strains that overexpress mutant JpsA or carry the vector ($JspA_{E148A}$ vs.
967 vector). The 141 genes that appeared in both the JspA vs. vector and JspA vs. $JspA_{E148A}$
968 comparisons were grouped according to their functions, as listed on the right. ChvI belongs to
969 the group of regulators whose gene expression increased when JspA was overexpressed. (B,
970 C) The bottom Venn diagrams represent the overlaps of (B) genes that belong to the JspA or
971 ExoR/ExoS transcriptome or ChvI regulon and (C) those that belong to the RpoH1 or JspA
972 transcriptome. Gene sets and analyses of their overlaps are provided in Tables S4 and S5.
973 See Materials and methods for details about assignment of genes to the ChvI regulon and
974 ExoR/ExoS transcriptome.
975
976
977 FIGURE 6. Epistatic interaction between *jspA* and *lppA* and the *exoR-exoS-chvI* pathway. (A)
978 Calcofluor fluorescence of wild-type and mutant strains were assessed by spotting ten-fold
979 serial dilutions of cultures onto LB plates. Strain genotypes are shown to the left of the
980 fluorescence images, while percentages on the right indicate averages (± standard deviations)
981 of fluorescence levels relative to the Rm1021 wild type, set as 100% on each plate.

Representative images are shown, and at least two replicates were included for each comparison. (B) Results from epistasis analysis, along with the predicted extracytoplasmic locations of JspA and LppA, suggest that they act upstream of the ExoR-ExoS-ChvI signaling pathway, as depicted by the schematic diagram. As a typical histidine kinase and response regulator, ExoS and ChvI are presumed to function as homodimers (Cheng & Walker, 1998b; Ratib *et al.*, 2018); for simplicity, the diagram does not show that. (C) Expression of the *exoY-uidA* reporter was monitored in strains replete with or depleted of ChvI, while *jspA* or $jspA_{E184A}$ was ectopically expressed. Relevant alleles on the chromosome and on plasmids are indicated below the plot: first row indicates the presence or absence of chromosomal *chvI* (+ or Δ), second row indicates presence of empty vector or a plasmid that expresses *chvI* (vector or +), and the third row indicates presence of vector or a plasmid that expresses wild-type or mutant *jspA* (vector, +, or E148A, respectively). Δ*chvI* strains (rightmost three strains) carried a complementing plasmid (pAD101) with *chvI* under the control of the P_{lac} promoter (P_{lac}-*chvI*): growth in the presence of absence of IPTG resulted in expression or depletion of ChvI. For comparison, $chvI^+$ strains carried the P_{lac}-*chvI* plasmid or the corresponding parent vector (pSRKKm). The strains also bore a compatible vector (pCM130) or its derivatives with taurine-regulated *jspA* or $jspA_{E184A}$ (pJC535 or pJC555). Strains were grown in LB with 10 mM taurine for 6 hours, while expressing or depleting ChvI, prior to measurement of GUS activities. Averages and standard deviations (error bars) were calculated with measurements from at least five different days. **, $p < 0.01$ between specified measurements.

FIGURE 7. Effects of *jspA* and *lppA* on transcriptional responses to pH shift. Changes in gene expression were determined using fusions of *uidA* (encoding the GUS reporter) to (A) SMb21188, (B) SMc01580, (C) SMb20946 (*exoY*), and (D) SMc02560 (*chvI*) at their native loci, generated in such a way as to preserve the function of the gene being examined. GUS activities in Rm1021 wild-type, Δ*jspA*, and Δ*lppA* strains were measured 4.5 hours after cultures were shifted from pH 7 to pH 6 (pink bars), 7 (yellow bars), or 8.5 (blue bars) in LB medium. Activity at pH 6 relative to pH 7 for each genotype is shown as the red percentage above each pink bar. Maroon * or ** within a bar for one of the mutants represents significant difference ($p < 0.05$ or $p < 0.01$, respectively) when compared to the same condition in wild type. Analogously, black * or ** indicates significant difference when activity at pH 6 or 8.5 is compared to that at pH 7 for the same genotype. Averages and standard deviations (error bars) were calculated from three to six independent measurements.

FIGURE 8. Effects of JspA on ExoR levels. (A) Plot depicts growth of *exoR-V5* strains carrying the pSRKGm vector or derivatives (pJC652 or pJC653) with *jspA* or *jspA*$_{E184A}$ (noted as E148A) under control of the P_{lac} promoter. Strains JOE5242, JOE5244, and JOE5246 were grown in 48-well plates, with 0.4 mL PYE plus 1 mM IPTG per well. Absorbance at 600 nm (A600) was measured every 30 minutes. Average readings for three different days are depicted, with surrounding shadings indicating standard deviations. In the absence of IPTG, all strains exhibited growth patterns similar to that of the vector-carrying strain in the presence of IPTG (see Fig. S4A). (B) Immunoblot shows steady-state levels of ExoR-V5 and the beta subunit of ATP synthase at 0, 3, and 6 hours after inducing expression of *jspA* or *jspA*$_{E184A}$, compared against levels in the vector-carrying strain. Approximate molecular mass, in kDa, are shown to the left of the blot, while lane numbers are shown below. Growth conditions were similar to that in (A), except that strains were cultured in flasks. (C) Expression of the *uidA* reporter fusion to *exoR* from its native locus was assessed in strains carrying the vector (pCM130) or overproducing JspA or JspA$_{E148A}$ (with pJC535 or pJC555). Strains were grown with 10 mM taurine for 4.5 hours prior to measurement of GUS activities. Averages and standard deviations were calculated from at least four measurements. *, $p < 0.05$ when compared against the vector-carrying strain.

FIGURE 9. Steady-state levels of ExoR-FLAG when *jspA* or *lppA* differentially expressed. (A) Levels of ExoR-FLAG in the presence of different versions of JspA were assessed by immunoblotting with anti-FLAG antibodies (bottom blot), while expression of JspA-HA was verified with anti-HA antibodies (top blot). ExoR-FLAG expression is indicated above the blots: + signifies that expression of ExoR-FLAG from pMB859 was induced with 0.5 mM IPTG in TY medium for 4.5 hours, while - signifies that the strain carried the empty vector pSRKKm under the same conditions. Presence (+) or deletion (Δ) of the native *jspA* in the chromosome is also indicated. Different versions of JspA were induced with 10 mM taurine as follows: wild-type JspA from pJC614 (black +), mutant JspA$_{E148A}$ from pJC615 (black *), wild-type JspA-HA from pJC616 (red +), mutant JspA$_{E148A}$-HA from pJC617 (red *), and no expression from the vector pJC473 (-). (B) Immunoblots show steady-state levels of ExoR-FLAG and JspA-HA in the presence or absence of chromosomal *lppA*. The presence (+) or deletion (Δ) of native *jspA* or *lppA* on the chromosome is shown above the blots. Expression of JspA-HA, wid-type (+) or

mutant (*), is indicated above the blots as in (A) (JspA-HA row). All strains in (B) expressed ExoR-FLAG from pMB859, induced with 0.5 mM IPTG. Approximate molecular mass, in kDa, are shown to the left of the blots, while lane numbers are shown below. Positions of bands representing JspA-HA and ExoR-FLAG are indicated to the right of the blots. Both sets of blots were first probed with anti-FLAG antibodies and then anti-HA antibodies (see Materials and methods). The bottom images were captured first, while the top images were acquired from the same respective blots after the second probing.

FIGURE 10. Steady-state levels of ExoR-FLAG when co-expressed with JspA and LppA in *C. crescentus* NA1000 or *E. coli* DH10B. (A) Levels of ExoR-FLAG and JspA-HA were assessed in NA1000 by immunoblotting with anti-FLAG and anti-HA antibodies. ExoR-FLAG expression is indicated above the blot: + signifies that expression of ExoR-FLAG from pMB859 was induced with 0.1 mM IPTG in PYE medium for 4 hours, while - signifies that the strain carried the empty vector pSRKKm under the same conditions. Expression of LppA and different versions of JspA were induced with 10 mM taurine from the following plasmids: lanes 1 and 2, pJC473 vector when neither expressed (- for both LppA and JspA); lane 3, pJC614 for JspA (black +); lane 4, pJC615 for $JspA_{E148A}$ (black *); lane 5, pJC702 for both LppA and JspA; lane 6, pJC706 for LppA and $JspA_{E148A}$; lane 7, pJC707 for LppA and JspA-HA (red +); and lane 8, pJC708 for LppA and $JspA_{E148A}$-HA (red *). (B) Immunoblots show steady-state levels of JspA-HA, LppA-HA, and ExoR-FLAG in DH10B. All strains were induced with 0.1 mM IPTG in LB medium for 4 hours. ExoR-FLAG expression is indicated above the blots: + signifies expression from pMB859, while - signifies carriage of the pSRKKm vector. Expression of different versions of JspA-HA and varying levels of LppA-HA was achieved using different plasmids, similarly indicated above the blots as in (A): lane 1, pDSW208 vector (expressing GFP); lanes 2 and 8, pJC720 (*jspA-HA* only); lanes 3 and 9, pJC733 ($jspA_{E148A}$-*HA*); lane 4, pJC730 (*jspA-HA* and *lppA-HA*, with intervening RBS); lane 5, pJC735 ($jspA_{E148A}$-*HA* and *lppA-HA*, with intervening RBS); lane 6, pJC731 (*jspA-HA* translationally coupled to *lppA-HA*); and lane 7, pJC736 ($jspA_{E148A}$-*HA* translationally coupled to *lppA-HA*). Higher levels of expression of LppA-HA in lanes 6 and 7 are represented by the larger, bold + sign above the blots. Blots were first probed with anti-FLAG antibodies and then with anti-HA antibodies. Approximate molecular mass, in kDa, are shown to the left of the blots, while lane numbers are shown below. Positions of bands representing JspA-HA, LppA-HA, and ExoR-FLAG are indicated to the right of the blots. Protein band designated by a red asterisk is presumed to be a fusion of JspA-HA and LppA-HA that

resulted from translational read-through. *E. coli* anti-HA images were captured from the same representative blot (with longer exposure for LppA-HA), while the anti-FLAG image was from a duplicate blot of the same samples.

Table 1. Expression levels of select promoters in wild type and deletion mutants, as measured by transcriptional fusions to the GUS reporter (encoded by *uidA*).

Promoter tested / Strain genotype	**LB**					**PYE**				
***exoY* (SMb20946)**										
Rm1021	8.7	±	2.0		**100%**	6.9	±	0.8		**100%**
Δ*jspA*	4.8	±	0.8	**	**55%**	4.4	±	1.0	**	**64%**
Δ*lppA*	5.6	±	1.5	*	**64%**	5.0	±	0.5	**	**72%**
Δ*jspA* Δ*lppA*	4.6	±	0.5	**	**52%**	4.0	±	0.5	**	**58%**
***flaC* (SMc03040)**										
Rm1021	4.4	±	0.5		**100%**	10.3	±	1.1		**100%**
Δ*jspA*	6.0	±	1.2	**	**136%**	11.8	±	0.9	*	**115%**
Δ*lppA*	5.9	±	1.0	**	**134%**	11.8	±	0.7	*	**114%**
Δ*jspA* Δ*lppA*	6.1	±	0.6	**	**140%**	12.2	±	1.4	*	**118%**
***mcpU* (SMc00975)**										
Rm1021	6.5	±	0.8		**100%**	52.8	±	7.7		**100%**
Δ*jspA*	10.4	±	0.9	**	**159%**	67.9	±	7.9	**	**129%**
Δ*lppA*	9.8	±	1.2	**	**149%**	61.8	±	11.2		**117%**
Δ*jspA* Δ*lppA*	10.4	±	1.4	**	**159%**	62.1	±	8.1		**118%**

β-glucuronidase (GUS) activities (averages ± standard deviations, in Miller units) of strains grown in LB or PYE were measured as described in Materials and methods. Averages and standard deviations were calculated from values obtained with at least five biological replicates. Percentage equals the enzymatic activity, expressed from the indicated promoter-*uidA* fusion, in the mutant divided by that in wild-type Rm1021. Two-tailed, unequal variances t-test was used to determine whether differences between wild-type and mutant strains were statistically significant: *, $0.01 < p < 0.05$; **, $p < 0.01$. Nonreplicating plasmids integrated into the genome to create transcriptional fusions to *exoY*, *flaC*, and *mcpU* were pEC340, pMB694, and pMB696, respectively.

Table 2. Activities of transcriptional fusion reporters when *jspA* or *lppA* ectopically expressed.

Condition / Strain genotype	**Promoter activity**				
PYE + 10 mM taurine, 3 hr	***flaC* (SMc03040)**				
Rm1021 / pCM130 (vector)	9.8	±	0.5		**100%**
Rm1021 / pJC535 (P_{tau}-***jspA***)	7.1	±	0.4	**	**72%**
Rm1021 / pJC532 (P_{tau}-***lppA***)	9.5	±	0.9		**98%**
	***exoY* (SMb20946)**				
Rm1021 / pCM130	7.3	±	0.6		**100%**
Rm1021 / pJC535 (P_{tau}-***jspA***)	14.6	±	0.8	**	**199%**
Rm1021 / pJC532 (P_{tau}-***lppA***)	8.2	±	0.5		**112%**
Δ*jspA* / pCM130	5.1	±	0.8	**	**69%**
Δ*jspA* / pJC535 (P_{tau}-***jspA***)	11.3	±	2.2	*	**155%**
Δ*lppA* / pCM130	5.4	±	1.3		**75%**
Δ*lppA* / pJC535 (P_{tau}-***jspA***)	6.2	±	1.7		**84%**
LB + 100 mM taurine, 6 hr	***exoY* (SMb20946)**				
Rm1021 / pCM130	9.0	±	0.5		**100%**
Rm1021 / pJC532 (P_{tau}-***lppA***)	10.6	±	0.7	*	**118%**
Δ*lppA* / pCM130	5.0	±	1.1	**	**56%**
Δ*lppA* / pJC532 (P_{tau}-***lppA***)	9.1	±	0.8		**102%**
Δ*jspA* / pCM130	4.7	±	0.8	**	**52%**
Δ*jspA* / pJC532 (P_{tau}-***lppA***)	4.8	±	0.6	**	**54%**

β-glucuronidase (GUS) activities (averages ± standard deviations, in Miller units) of strains grown under the indicated conditions were measured as described in Materials and methods. Averages and standard deviations were calculated from values obtained with at least three biological replicates. Percentages equal the enzymatic activities, expressed from the indicated promoter-*uidA* fusions, of the respective strains divided by that in wild-type Rm1021 carrying the pCM130 vector. Two-tailed, unequal variances t-test was used to determine whether differences from the vector-carrying wild type were statistically significant: *, $0.01 < p < 0.05$; **, $p < 0.01$. Nonreplicating plasmids integrated into the genome to create transcriptional fusions to *exoY* and *flaC* were pEC340 and pMB694, respectively.

Table 3. Expression from reporter fusion to *exoY* promoter when mutant *jspA* or *lppA* allele overexpressed.

Strain genotype	***exoY* (SMb20946) expression**				
Overexpress *jspA* alleles	**PYE + 10 mM tau, 4.5 hrs**				
Rm1021 / pCM130 (vector)	7.5	±	1.5		**100%**
Rm1021 / pJC535 (P_{tau}-***jspA***)	17.8	±	3.7	**	**238%**
Rm1021 / pJC555 (P_{tau}-***jspA*$_{E148A}$**)	8.4	±	0.4	*	**113%**
Rm1021 / pJC556 (P_{tau}-***jspA*$_{E148D}$**)	8.4	±	1.0		**112%**
Rm1021 / pJC558 (P_{tau}-***jspA-HA***)	11.8	±	1.7	**	**158%**
Rm1021 / pJC559 (P_{tau}-***jspA*$_{E148A}$-*HA***)	7.1	±	1.6		**96%**
Rm1021 / pJC560 (P_{tau}-***jspA*$_{E148D}$-*HA***)	6.8	±	0.8		**90%**
Δ*jspA* / pJC558 (P_{tau}-***jspA-HA***)	10.9	±	1.4	**	**146%**
Δ*lppA* / pJC558 (P_{tau}-***jspA-HA***)	7.0	±	1.2		**93%**
Overexpress *lppA* alleles	**LB + 100 mM tau, 6 hrs**				
Δ*lppA* / pCM130	6.1	±	0.6		**100%**
Δ*lppA* / pJC532 (P_{tau}-***lppA***)	11.9	±	1.1	**	**195%**
Δ*lppA* / pJC605 (P_{tau}-***lppA*$_{C23S}$**)	7.0	±	0.7		**115%**
Δ*lppA* / pJC606 (P_{tau}-***lppA-HA***)	11.0	±	1.3	**	**180%**
Δ*lppA* / pJC607 (P_{tau}-***lppA*$_{C23S}$-*HA***)	6.8	±	1.0		**111%**
Δ*lppA* / pJC608 (P_{tau}-***lppA*$_{G96W}$-*HA***)	8.8	±	0.4	**	**130%**
Δ*lppA* / pJC609 (P_{tau}-***lppA*$_{A78S}$-*HA***)	8.3	±	0.3	**	**123%**

β-glucuronidase (GUS) activities (in Miller units) of strains grown under the indicated conditions were measured as described in Materials and methods. Averages and standard deviations were derived from values obtained with at least three biological replicates. Averages for the vector-carrying wild type and *lppA* deletion mutant (first line of each group) were set at 100% and used to calculate relative activities. Statistical significance of differences from the vector-carrying wild type or *lppA* deletion mutant was determined with t-test (two-tailed, unequal variances): *, $0.01 < p < 0.05$; **, $p < 0.01$. Nonreplicating plasmid pEC340 was integrated into the genomes of different strains to generate transcriptional fusion to *exoY*.

Table 4. Select promoters confirm transcriptional changes when *jspA* overexpressed.

Promoter tested / Strain genotype	**GUS activity**				**% WT**
***mcpU* (SMc00975)**	**PYE + 10 mM tau, 4.5 hrs**				
Rm1021 / pCM130 (vector)	40.0	±	3.7		**100%**
Rm1021 / pJC535 (P_{tau}-***jspA***)	25.3	±	2.7	*	**63%**
Rm1021 / pJC555 (P_{tau}-***jspA*$_{E148A}$**)	39.2	±	2.0		**98%**
SMc01580					
Rm1021 / pCM130	6.3	±	1.2		**100%**
Rm1021 / pJC535 (P_{tau}-***jspA***)	20.3	±	1.1	**	**321%**
Rm1021 / pJC555 (P_{tau}-***jspA*$_{E148A}$**)	7.1	±	0.6		**113%**
***pckA* (SMc02562)**					
Rm1021 / pCM130	38.4	±	9.4		**100%**
Rm1021 / pJC535 (P_{tau}-***jspA***)	59.1	±	8.7	**	**154%**
Rm1021 / pJC555 (P_{tau}-***jspA*$_{E148A}$**)	45.5	±	12.6		**119%**
***chvI* (SMc02560)**					
Rm1021 / pCM130	20.4	±	2.8		**100%**
Rm1021 / pJC535 (P_{tau}-***jspA***)	39.3	±	6.7	**	**193%**
Rm1021 / pJC555 (P_{tau}-***jspA*$_{E148A}$**)	23.5	±	3.3		**115%**
***chvI* (SMc02560)**	**PYE + 1 mM IPTG, 4.5 hrs**				
Rm1021 / pSRKGm	27.1	±	1.5		**100%**
Rm1021 / pJC652 (P_{lac}-***jspA***)	43.2	±	7.0	**	**159%**
Rm1021 / pJC653 (P_{lac}-***jspA*$_{E148A}$**)	30.8	±	4.5		**114%**
Rm1021 / pJC654 (P_{lac}-***jspA-HA***)	41.2	±	3.6	**	**152%**
Rm1021 / pJC655 (P_{lac}-***jspA*$_{E148A}$*-HA***)	31.4	±	2.8	*	**116%**

β-glucuronidase (GUS) activities (in Miller units) of strains grown under the indicated conditions were measured as described in Materials and methods. Averages and standard deviations were derived from values obtained with at least three biological replicates. Averages for the vector-carrying wild type (first line of each group) were set at 100% and used to calculate relative activities (% WT). Statistical significance of differences from the vector-carrying wild type was determined with t-test (two-tailed, unequal variances): *, $0.01 < p < 0.05$; **, $p < 0.01$. Nonreplicating plasmids integrated into the genome to create transcriptional fusions of *uidA* to *mcpU*, SMc01580, *pckA*, and *chvI* were pMB696, pJC640, pJC639, and pJC638, respectively.

Supporting information

S1 Fig. Production of calcofluor-binding exopolysaccharides in *S. medicae* WSM419 and its derivatives. Ten-fold serial dilutions of logarithmic-phase cultures were spotted onto solid media and allowed to grow for three days prior to imaging. (A) Representative images show fluorescence of wild-type WSM419, Δ*jspA* (ΔSmed_3110) mutant, Δ*lppA* (ΔSmed_0632) mutant, and derivatives marked with neomycin (Nm^R) or spectinomycin (Sp^R) resistance [*nptII* or *aadA* linked to *podJ* (Smed_0147) or replacing *jspA*] on LB plates containing calcofluor. Darker spots indicate brighter fluorescence. (B) WSM, Δ*jspA*, and Δ*lppA* strains carrying the vector (pCM130) or a plasmid with *S. meliloti jspA*, $jspA_{E148A}$, or *lppA* under the control of a taurine-inducible promoter (pJC535, pJC555, or pJC532, respectively) were grown on LB plates containing tetracycline (Tet) and calcofluor, without or with taurine (5 mM taurine for *jspA* complementation, 10 mM for *lppA*). Visible-light images of corresponding strains grown on PYE plates show mucoid colonies. Labels on the left indicate strain numbers, while labels on the right indicate genotypes. Each experiment was performed at least twice.

S2 Fig. Overexpression of *jspA* alleles in *S. medicae* WSM419, *S. fredii* NGR234, and *C. crescentus* NA1000. Ten-fold serial dilutions of logarithmic-phase cultures were spotted onto PYE plates containing 0, 5, or 10 mM taurine. NA1000 strains were grown with 1 μg/mL oxytetracycline for two days, while WSM419 and NGR234 strains were grown with 5 μg/mL oxytetracycline for three days at 30°C prior to imaging. Labels on the left indicate strain numbers, while labels on the right indicate the *jspA* alleles being expressed from a plasmid. Plasmids used were pJC614 (*jspA*), pJC615 ($jspA_{E148A}$), pJC616 (*jspA-HA*), and pJC617 ($jspA_{E148A}$-*HA*). Images shown represent four replicates on two different days.

S3 Fig. Depletion of ChvI. (A) Plate images show growth of ChvI depletion strain on LB medium in the presence and absence of 1 mM IPTG. The top strain (AD124) carried the pSRKKm vector and had a Δ*chvI* allelic replacement plasmid (pAD112) integrated into its chromosome but retained a copy of $chvI^+$, while the bottom strain (AD115) carried pAD101, with *chvI* under the control of the P_{lac} promoter, and had its *chvI* replaced by a hygromycin resistance gene (*hph*). (B) Plots show growth curves of ChvI depletion strains over 24 hours in LB, in the presence or absence of 0.5 mM IPTG. $chvI^+$ or Δ*chvI* strains carried pAD101, as well as a compatible vector (pCM130) or derivatives (pJC535 or pJC555) containing taurine-regulated

jspA or *jspA*$_{E184A}$ (abbreviated as E148A), under control of the P_{tau} promoter. No taurine was added in these growth experiments. Cultures were shaken at 1000 rpm in 48-well plates, with 0.4 mL medium (containing kanamycin and oxytetracycline) per well. Absorbance at 600 nm (A600) was measured every 30 minutes. Average readings for three different days are shown, with corresponding shadings indicating standard deviations. In the presence of IPTG, all strains exhibited similar growth patterns; curves for depletion strains carrying P_{tau}-*jspA* or *jspA*$_{E148A}$ grown with IPTG were omitted for clarity. Strains shown here for growth curves (JOE5579, JOE5605, JOE5607, JOE5609) all contain a genomic *exoY-uidA* reporter and constitute a subset of those used for GUS assays in Figure 6C.

S4 Fig. Growth curves of *exoR-V5* strains carrying the pSRKGm vector or derivatives (pJC652 or pJC653) with *jspA* or *jspA*$_{E184A}$ (noted as E148A) under control of the P_{lac} promoter. (A) Strains JOE5242, JOE5244, and JOE5246 were grown in 48-well plates, with 0.4 mL PYE per well, in the presence of absence of 1 mM IPTG. Absorbance at 600 nm (A600) was measured every 30 minutes. Average readings for three different days are depicted, with surrounding shadings indicating standard deviations. Lines without markers represent growth in the absence of IPTG (-); standard deviations for these were omitted for simplicity. Figure 7 shows a portion of this graph. (B, C) Liquid cultures of the same strains were grown in flasks with 1 mM IPTG in (B) PYE or (C) LB medium, and A600 was measured every hour for 12 hours. The plots were generated from single experiments.

S5 Fig. Steady-state levels of ExoR-FLAG when co-expressed with different forms of JspA and varying levels of LppA in *C. crescentus* NA1000 or *E. coli* DH10B. (A) Levels of ExoR-FLAG and JspA-HA were assessed in NA1000 by immunoblotting with anti-FLAG and anti-HA antibodies. ExoR-FLAG expression is indicated above the blot: + signifies that expression of ExoR-FLAG from pMB859 was induced with 0.1 mM IPTG in PYE medium for 4 hours, while - signifies that the strain carried the empty vector pSRKKm under the same conditions. Expression of LppA and different versions of JspA were induced with 10 mM taurine from the following plasmids: lanes 1 and 4, pJC473 vector when neither expressed (- for both LppA and JspA); lanes 2 and 9, pJC616 for JspA-HA only (red +); lanes 3 and 10, pJC617 for JspA$_{E148A}$-HA (red *); lane 5, pJC614 for JspA (black +); lane 6, pJC615 for JspA$_{E148A}$ (black *); lane 7, pJC702 for LppA and JspA; lane 8, pJC706 for LppA and JspA$_{E148A}$; lane 11, pJC707 for LppA and JspA-HA; and lane12, pJC708 for LppA and JspA$_{E148A}$-HA. (B) Immunoblots show steady-state levels of JspA-HA, LppA-HA, and ExoR-FLAG in DH10B. All strains were induced

with 0.1 mM IPTG in LB medium for 4 hours. ExoR-FLAG expression is indicated above the blots: + signifies expression from pMB859, while - signifies carriage of the pSRKKm vector. Expression of different versions of JspA-HA and varying levels of LppA-HA was achieved using different plasmids, similarly indicated above the blots as in (A): lane 1 and 14, pDSW208 vector (expressing GFP); lanes 2 and 10, pJC720 (*jspA-HA* only); lanes 3 and 11, pJC733 ($jspA_{E148A}$-*HA*); lane 4, pJC730 (*jspA-HA* and *lppA-HA*, with intervening RBS); lane 5, pJC735 ($jspA_{E148A}$-*HA* and *lppA-HA*, with intervening RBS); lane 6, pJC731 (*jspA-HA* translationally coupled to *lppA-HA*); lane 7, pJC736 ($jspA_{E148A}$-*HA* translationally coupled to *lppA-HA*); lanes 8 and12, pJC734 (*lppA-HA* followed by *jspA-HA*); and lanes 9 and 13, pJC737 (*lppA-HA* followed by $jspA_{E148A}$-*HA*). Schematics above the blots represent gene arrangements on plasmids: red * indicates plasmids that carry the $jspA_{E148A}$-*HA* mutant allele and the approximate location of the active site mutation in the gene; RBS preceding *lppA-HA* in pJC730 and pJC735 is the ribosome binding site of *E. coli araB*. Lanes 1 - 7 have the same configuration of strains as those in Figure 9B. The size of the + symbol in the LppA-HA row above the blots reflects the level of expression, with the orange, bold + indicating the highest levels. (LppA-HA is not detectable in some lanes because the signal is overwhelmed by that in lanes with high expression.) Approximate molecular mass, in kDa, are shown to the left of the blots, while lane numbers are shown below. Positions of bands representing JspA-HA, LppA-HA, and ExoR-FLAG are indicated to the right of the blots. Blots were first probed with anti-FLAG antibodies and then with anti-HA antibodies. The ExoR-FLAG image was captured first, and the JspA-HA image was obtained from the same representative blot after the second probing, while the LppA-HA image was acquired from a duplicate blot of the same samples.

S1 Table. Orthologs of JspA, LppA, and ExoR in representative bacterial species.

S2 Table. Number of pink and white nodules on individual *M. sativa* or *M. truncatula* seedlings inoculated with Rm1021 or WSM419 strains.

S3 Table. Compilations of symbiosis competitions between Rm1021 strains in *M. sativa* or between WSM419 strains in *M. truncatula*.

S4 Table. JspA-regulated genes.

S5 Table. Hypergeometric probability tests for overlaps between JspA, ExoRS, and RpoH1 transcriptomes and ChvI regulon.

S6 Table. Hypergeometric probability tests for overlap of JspA transcriptome with genes that altered expression in NCR247-treated cells or the Δ*podJ1* mutant.

S7 Table. Overlap of JspA transcriptome with genes that changed expression upon acid stress.

S8 Table. *Sinorhizobium* strains used in this study.

S9 Table. Plasmids used in this study.

S1 File. Plasmid sequences.

References

Alakavuklar, M.A., Fiebig, A., and Crosson, S. (2023) The *Brucella* Cell Envelope. *Annu Rev Microbiol*.

Alakavuklar, M.A., Heckel, B.C., Stoner, A.M., Stembel, J.A., and Fuqua, C. (2021) Motility control through an anti-activation mechanism in *Agrobacterium tumefaciens*. *Mol Microbiol* **116**: 1281-1297.

Alba, B.M., Leeds, J.A., Onufryk, C., Lu, C.Z., and Gross, C.A. (2002) DegS and YaeL participate sequentially in the cleavage of RseA to activate the sigma(E)-dependent extracytoplasmic stress response. *Genes Dev* **16**: 2156-2168.

Albicoro, F.J., Draghi, W.O., Martini, M.C., Salas, M.E., Torres Tejerizo, G.A., Lozano, M.J., Lopez, J.L., Vacca, C., Cafiero, J.H., Pistorio, M., Bednarz, H., Meier, D., Lagares, A., Niehaus, K., Becker, A., and Del Papa, M.F. (2021) The two-component system ActJK is involved in acid stress tolerance and symbiosis in *Sinorhizobium meliloti*. *J Biotechnol* **329**: 80-91.

Albicoro, F.J., Vacca, C., Cafiero, J.H., Draghi, W.O., Martini, M.C., Goulian, M., Lagares, A., and Del Papa, M.F. (2023) Comparative Proteomic Analysis Revealing ActJ-Regulated Proteins in *Sinorhizobium meliloti*. *J Proteome Res*.

Altamirano-Silva, P., Cordero-Serrano, M., Méndez-Montoya, J., Chacón-Díaz, C., Guzmán-Verri, C., Moreno, E., and Chaves-Olarte, E. (2021) Intracellular Passage Triggers a Molecular Response in *Brucella abortus* That Increases Its Infectiousness. *Infection and Immunity* **89**: e00004-00021.

Altamirano-Silva, P., Meza-Torres, J., Castillo-Zeledon, A., Ruiz-Villalobos, N., Zuniga-Pereira, A.M., Chacon-Diaz, C., Moreno, E., Guzman-Verri, C., and Chaves-Olarte, E. (2018) *Brucella abortus* senses the intracellular environment through the BvrR/BvrS two-component system, which allows *B. abortus* to adapt to its replicative niche. *Infect Immun* **86**.

An, F., Li, N., Zhang, L., Zheng, W., Xing, S., Tang, G., Yan, J., Yu, L., and Luo, L. (2021) Identification of *Sinorhizobium meliloti* LsrB regulon. *Acta biochimica et biophysica Sinica* **53**: 955-957.

Arnold, M.F.F., Penterman, J., Shabab, M., Chen, E.J., and Walker, G.C. (2018) Important Late-Stage Symbiotic Role of the *Sinorhizobium meliloti* Exopolysaccharide Succinoglycan. *J Bacteriol* **200**.

Arnold, M.F.F., Shabab, M., Penterman, J., Boehme, K.L., Griffitts, J.S., and Walker, G.C. (2017) Genome-Wide Sensitivity Analysis of the Microsymbiont *Sinorhizobium meliloti* to Symbiotically Important, Defensin-Like Host Peptides. *mBio* **8**.

Ausubel, F.M., Brent, R., Kingston, R.E., Moore, D.D., Seidman, J.G., Smith, J.A., and Struhl, K., (1998) *Current Protocols in Molecular Biology*. John Wiley & Sons, New York, NY.

Bahlawane, C., McIntosh, M., Krol, E., and Becker, A. (2008) *Sinorhizobium meliloti* regulator MucR couples exopolysaccharide synthesis and motility. *Mol Plant Microbe Interact* **21**: 1498-1509.

Baraquet, C., Dai, W., Mendiola, J., Pechter, K., and Harwood, C.S. (2021) Transposon sequencing analysis of *Bradyrhizobium diazoefficiens* 110*spc*4. *Scientific reports* **11**: 13211.

Barnett, M.J., Bittner, A.N., Toman, C.J., Oke, V., and Long, S.R. (2012) Dual RpoH sigma factors and transcriptional plasticity in a symbiotic bacterium. *J Bacteriol* **194**: 4983-4994.

Barnett, M.J., and Fisher, R.F. (2006) Global gene expression in the rhizobial-legume symbiosis. *Symbiosis* **42**: 1-24.

Barnett, M.J., and Long, S.R. (2015) The *Sinorhizobium meliloti* SyrM regulon: effects on global gene expression are mediated by *syrA* and *nodD3*. *J Bacteriol* **197**: 1792-1806.

Barnett, M.J., and Long, S.R. (2018) Novel Genes and Regulators That Influence Production of Cell Surface Exopolysaccharides in *Sinorhizobium meliloti*. *J Bacteriol* **200**.

Barnett, M.J., Oke, V., and Long, S.R. (2000) New genetic tools for use in the *Rhizobiaceae* and other bacteria. *Biotechniques* **29**: 240-242, 244-245.

1321 Barnett, M.J., Solow-Cordero, D.E., and Long, S.R. (2019) A high-throughput system to identify inhibitors
1322 of *Candidatus* Liberibacter asiaticus transcription regulators. *Proc Natl Acad Sci U S A* **116**:
1323 18009-18014.
1324 Barnett, M.J., Toman, C.J., Fisher, R.F., and Long, S.R. (2004) A dual-genome Symbiosis Chip for
1325 coordinate study of signal exchange and development in a prokaryote-host interaction. *Proc*
1326 *Natl Acad Sci USA* **101**: 16636-16641.
1327 Barrett, T., Wilhite, S.E., Ledoux, P., Evangelista, C., Kim, I.F., Tomashevsky, M., Marshall, K.A., Phillippy,
1328 K.H., Sherman, P.M., Holko, M., Yefanov, A., Lee, H., Zhang, N., Robertson, C.L., Serova, N.,
1329 Davis, S., and Soboleva, A. (2013) NCBI GEO: archive for functional genomics data sets--update.
1330 *Nucleic Acids Res* **41**: D991-995.
1331 Becker, A., Barnett, M.J., Capela, D., Dondrup, M., Kamp, P.B., Krol, E., Linke, B., Ruberg, S., Runte, K.,
1332 Schroeder, B.K., Weidner, S., Yurgel, S.N., Batut, J., Long, S.R., Pühler, A., and Goesmann, A.
1333 (2009) A portal for rhizobial genomes: RhizoGATE integrates a *Sinorhizobium meliloti* genome
1334 annotation update with postgenome data. *J Biotechnol* **140**: 45-50.
1335 Becker, A., Ruberg, S., Baumgarth, B., Bertram-Drogatz, P.A., Quester, I., and Puhler, A. (2002)
1336 Regulation of succinoglycan and galactoglucan biosynthesis in *Sinorhizobium meliloti*. *J Mol*
1337 *Microbiol Biotechnol* **4**: 187-190.
1338 Bélanger, L., Dimmick, K.A., Fleming, J.S., and Charles, T.C. (2009) Null mutations in *Sinorhizobium*
1339 *meliloti exoS* and *chvI* demonstrate the importance of this two-component regulatory system for
1340 symbiosis. *Mol Microbiol* **74**: 1223-1237.
1341 Benedict, A.B., Ghosh, P., Scott, S.M., and Griffitts, J.S. (2021) A conserved rhizobial peptidase that
1342 interacts with host-derived symbiotic peptides. *Scientific reports* **11**: 11779.
1343 Bensig, E.O., Valadez-Cano, C., Kuang, Z., Freire, I.R., Reyes-Prieto, A., and MacLellan, S.R. (2022) The
1344 two-component regulatory system CenK-CenR regulates expression of a previously
1345 uncharacterized protein required for salinity and oxidative stress tolerance in *Sinorhizobium*
1346 *meliloti*. *Front Microbiol* **13**: 1020932.
1347 Blum, M., Chang, H.Y., Chuguransky, S., Grego, T., Kandasaamy, S., Mitchell, A., Nuka, G., Paysan-
1348 Lafosse, T., Qureshi, M., Raj, S., Richardson, L., Salazar, G.A., Williams, L., Bork, P., Bridge, A.,
1349 Gough, J., Haft, D.H., Letunic, I., Marchler-Bauer, A., Mi, H., Natale, D.A., Necci, M., Orengo, C.A.,
1350 Pandurangan, A.P., Rivoire, C., Sigrist, C.J.A., Sillitoe, I., Thanki, N., Thomas, P.D., Tosatto, S.C.E.,
1351 Wu, C.H., Bateman, A., and Finn, R.D. (2021) The InterPro protein families and domains
1352 database: 20 years on. *Nucleic Acids Res* **49**: D344-D354.
1353 Boratyn, G.M., Camacho, C., Cooper, P.S., Coulouris, G., Fong, A., Ma, N., Madden, T.L., Matten, W.T.,
1354 McGinnis, S.D., Merezhuk, Y., Raytselis, Y., Sayers, E.W., Tao, T., Ye, J., and Zaretskaya, I. (2013)
1355 BLAST: a more efficient report with usability improvements. *Nucleic Acids Res* **41**: W29-33.
1356 Brockhurst, M.A. (2011) Sex, death, and the Red Queen. *Science* **333**: 166-167.
1357 Budnick, J.A., Sheehan, L.M., Ginder, M.J., Failor, K.C., Perkowski, J.M., Pinto, J.F., Kohl, K.A., Kang, L.,
1358 Michalak, P., Luo, L., Heindl, J.E., and Caswell, C.C. (2020) A central role for the transcriptional
1359 regulator VtlR in small RNA-mediated gene regulation in *Agrobacterium tumefaciens*. *Scientific*
1360 *reports* **10**: 14968.
1361 Burks, D., Azad, R., Wen, J., and Dickstein, R. (2018) The *Medicago truncatula* Genome: Genomic Data
1362 Availability. *Methods Mol Biol* **1822**: 39-59.
1363 Calatrava-Morales, N., Nogales, J., Ameztoy, K., van Steenbergen, B., and Soto, M.J. (2017) The
1364 NtrY/NtrX System of *Sinorhizobium meliloti* GR4 Regulates Motility, EPS I Production, and
1365 Nitrogen Metabolism but Is Dispensable for Symbiotic Nitrogen Fixation. *Mol Plant Microbe*
1366 *Interact* **30**: 566-577.
1367 Cao, P., and Wall, D. (2020) The Fluidity of the Bacterial Outer Membrane Is Species Specific: Bacterial
1368 Lifestyles and the Emergence of a Fluid Outer Membrane. *Bioessays* **42**: e1900246.

1369 Cao, Y., Halane, M.K., Gassmann, W., and Stacey, G. (2017) The Role of Plant Innate Immunity in the
1370 Legume-Rhizobium Symbiosis. *Annu Rev Plant Biol* **68**: 535-561.
1371 Carroll, L., (1900 [1872]) *Through the Looking-Glass, and What Alice Found There*. W. B. Conkey Co.,
1372 Chicago.
1373 Castillo-Zeledón, A., Ruiz-Villalobos, N., Altamirano-Silva, P., Chacón-Díaz, C., Barquero-Calvo, E., Chaves-
1374 Olarte, E., and Guzmán-Verri, C. (2021) A *Sinorhizobium meliloti* and *Agrobacterium tumefaciens*
1375 ExoR ortholog is not crucial for *Brucella abortus* virulence. *PLoS One* **16**: e0254568.
1376 Charles, T.C., and Nester, E.W. (1993) A chromosomally encoded two-component sensory transduction
1377 system is required for virulence of *Agrobacterium tumefaciens*. *J Bacteriol* **175**: 6614-6625.
1378 Chen, E.J., Fisher, R.F., Perovich, V.M., Sabio, E.A., and Long, S.R. (2009) Identification of direct
1379 transcriptional target genes of ExoS/ChvI two-component signaling in *Sinorhizobium meliloti*. *J*
1380 *Bacteriol* **191**: 6833-6842.
1381 Chen, E.J., Sabio, E.A., and Long, S.R. (2008) The periplasmic regulator ExoR inhibits ExoS/ChvI two-
1382 component signalling in *Sinorhizobium meliloti*. *Mol Microbiol* **69**: 1290-1303.
1383 Cheng, H.P., and Walker, G.C. (1998a) Succinoglycan is required for initiation and elongation of infection
1384 threads during nodulation of alfalfa by Rhizobium meliloti. *J Bacteriol* **180**: 5183-5191.
1385 Cheng, H.P., and Walker, G.C. (1998b) Succinoglycan production by *Rhizobium meliloti* is regulated
1386 through the ExoS-ChvI two-component regulatory system. *J Bacteriol* **180**: 20-26.
1387 Crook, M.B., Lindsay, D.P., Biggs, M.B., Bentley, J.S., Price, J.C., Clement, S.C., Clement, M.J., Long, S.R.,
1388 and Griffitts, J.S. (2012) Rhizobial plasmids that cause impaired symbiotic nitrogen fixation and
1389 enhanced host invasion. *Mol Plant Microbe Interact* **25**: 1026-1033.
1390 Davies, B.W., and Walker, G.C. (2007) Identification of novel *Sinorhizobium meliloti* mutants
1391 compromised for oxidative stress protection and symbiosis. *J Bacteriol* **189**: 2110-2113.
1392 De Las Peñas, A., Connolly, L., and Gross, C.A. (1997) SigmaE is an essential sigma factor in *Escherichia*
1393 *coli*. *J Bacteriol* **179**: 6862-6864.
1394 de Lucena, D.K., Pühler, A., and Weidner, S. (2010) The role of sigma factor RpoH1 in the pH stress
1395 response of *Sinorhizobium meliloti*. *BMC Microbiol* **10**: 265.
1396 diCenzo, G.C., Benedict, A.B., Fondi, M., Walker, G.C., Finan, T.M., Mengoni, A., and Griffitts, J.S. (2018)
1397 Robustness encoded across essential and accessory replicons of the ecologically versatile
1398 bacterium *Sinorhizobium meliloti*. *PLoS Genet* **14**: e1007357.
1399 Doherty, D., Leigh, J.A., Glazebrook, J., and Walker, G.C. (1988) Rhizobium meliloti mutants that
1400 overproduce the *R. meliloti* acidic calcofluor-binding exopolysaccharide. *J Bacteriol* **170**: 4249-
1401 4256.
1402 Draghi, W.O., Del Papa, M.F., Hellweg, C., Watt, S.A., Watt, T.F., Barsch, A., Lozano, M.J., Lagares, A., Jr.,
1403 Salas, M.E., López, J.L., Albicoro, F.J., Nilsson, J.F., Torres Tejerizo, G.A., Luna, M.F., Pistorio, M.,
1404 Boiardi, J.L., Pühler, A., Weidner, S., Niehaus, K., and Lagares, A. (2016) A consolidated analysis
1405 of the physiologic and molecular responses induced under acid stress in the legume-symbiont
1406 model-soil bacterium *Sinorhizobium meliloti*. *Scientific reports* **6**: 29278.
1407 Eisfeld, J., Kraus, A., Ronge, C., Jagst, M., Brandenburg, V.B., and Narberhaus, F. (2021) A LysR-type
1408 transcriptional regulator controls the expression of numerous small RNAs in *Agrobacterium*
1409 *tumefaciens*. *Mol Microbiol* **116**: 126-139.
1410 Evinger, M., and Agabian, N. (1977) Envelope-associated nucleoid from *Caulobacter crescentus* stalked
1411 and swarmer cells. *J Bacteriol* **132**: 294-301.
1412 Fang, F.C., Frawley, E.R., Tapscott, T., and Vázquez-Torres, A. (2016) Bacterial Stress Responses during
1413 Host Infection. *Cell Host Microbe* **20**: 133-143.
1414 Farkas, A., Maroti, G., Durgo, H., Gyorgypal, Z., Lima, R.M., Medzihradszky, K.F., Kereszt, A., Mergaert, P.,
1415 and Kondorosi, E. (2014) *Medicago truncatula* symbiotic peptide NCR247 contributes to

1416 bacteroid differentiation through multiple mechanisms. *Proc Natl Acad Sci U S A* **111**: 5183-
1417 5188.
1418 Ferguson, B.J., Indrasumunar, A., Hayashi, S., Lin, M.H., Lin, Y.H., Reid, D.E., and Gresshoff, P.M. (2010)
1419 Molecular analysis of legume nodule development and autoregulation. *J Integr Plant Biol* **52**: 61-
1420 76.
1421 Fields, A.T., Navarrete, C.S., Zare, A.Z., Huang, Z., Mostafavi, M., Lewis, J.C., Rezaeihaghighi, Y., Brezler,
1422 B.J., Ray, S., Rizzacasa, A.L., Barnett, M.J., Long, S.R., Chen, E.J., and Chen, J.C. (2012) The
1423 conserved polarity factor *podJ1* impacts multiple cell envelope-associated functions in
1424 *Sinorhizobium meliloti*. *Mol Microbiol* **84**: 892-920.
1425 Finan, T.M., Hirsch, A.M., Leigh, J.A., Johansen, E., Kuldau, G.A., Deegan, S., Walker, G.C., and Signer, E.R.
1426 (1985) Symbiotic mutants of *Rhizobium meliloti* that uncouple plant from bacterial
1427 differentiation. *Cell* **40**: 869-877.
1428 Finan, T.M., Kunkel, B., De Vos, G.F., and Signer, E.R. (1986) Second symbiotic megaplasmid in *Rhizobium*
1429 *meliloti* carrying exopolysaccharide and thiamine synthesis genes. *J Bacteriol* **167**: 66-72.
1430 Flores-Tinoco, C.E., Tschan, F., Fuhrer, T., Margot, C., Sauer, U., Christen, M., and Christen, B. (2020) Co-
1431 catabolism of arginine and succinate drives symbiotic nitrogen fixation. *Molecular systems*
1432 *biology* **16**: e9419.
1433 Frohlich, K.S., Forstner, K.U., and Gitai, Z. (2018) Post-transcriptional gene regulation by an Hfq-
1434 independent small RNA in *Caulobacter crescentus*. *Nucleic Acids Res* **46**: 10969-10982.
1435 Fujimura-Kamada, K., Nouvet, F.J., and Michaelis, S. (1997) A novel membrane-associated
1436 metalloprotease, Ste24p, is required for the first step of NH2-terminal processing of the yeast a-
1437 factor precursor. *J Cell Biol* **136**: 271-285.
1438 Gage, D.J. (2002) Analysis of infection thread development using Gfp- and DsRed-expressing
1439 *Sinorhizobium meliloti*. *J Bacteriol* **184**: 7042-7046.
1440 Galibert, F., Finan, T.M., Long, S.R., Pühler, A., Abola, P., Ampe, F., Barloy-Hubler, F., Barnett, M.J.,
1441 Becker, A., Boistard, P., Bothe, G., Boutry, M., Bowser, L., Buhrmester, J., Cadieu, E., Capela, D.,
1442 Chain, P., Cowie, A., Davis, R.W., Dreano, S., Federspiel, N.A., Fisher, R.F., Gloux, S., Godrie, T.,
1443 Goffeau, A., Golding, B., Gouzy, J., Gurjal, M., Hernandez-Lucas, I., Hong, A., Huizar, L., Hyman,
1444 R.W., Jones, T., Kahn, D., Kahn, M.L., Kalman, S., Keating, D.H., Kiss, E., Komp, C., Lelaure, V.,
1445 Masuy, D., Palm, C., Peck, M.C., Pohl, T.M., Portetelle, D., Purnelle, B., Ramsperger, U., Surzycki,
1446 R., Thebault, P., Vandenbol, M., Vorholter, F.J., Weidner, S., Wells, D.H., Wong, K., Yeh, K.C., and
1447 Batut, J. (2001) The composite genome of the legume symbiont *Sinorhizobium meliloti*. *Science*
1448 **293**: 668-672.
1449 Geddes, B.A., Gonzalez, J.E., and Oresnik, I.J. (2014) Exopolysaccharide production in response to
1450 medium acidification is correlated with an increase in competition for nodule occupancy. *Mol*
1451 *Plant Microbe Interact* **27**: 1307-1317.
1452 Geiger, O., Sohlenkamp, C., Vera-Cruz, D., Medeot, D.B., Martínez-Aguilar, L., Sahonero-Canavesi, D.X.,
1453 Weidner, S., Pühler, A., and López-Lara, I.M. (2021) ExoS/ChvI Two-Component Signal-
1454 Transduction System Activated in the Absence of Bacterial Phosphatidylcholine. *Frontiers in*
1455 *Plant Science* **12**: 678976.
1456 Ghosh, P., Adolphsen, K.N., Yurgel, S.N., and Kahn, M.L. (2021) *Sinorhizobium medicae* WSM419 Genes
1457 That Improve Symbiosis between *Sinorhizobium meliloti* Rm1021 and *Medicago truncatula*
1458 Jemalong A17 and in Other Symbiosis Systems. *Appl Environ Microbiol* **87**: e0300420.
1459 Gibson, K.E., Barnett, M.J., Toman, C.J., Long, S.R., and Walker, G.C. (2007) The symbiosis regulator CbrA
1460 modulates a complex regulatory network affecting the flagellar apparatus and cell envelope
1461 proteins. *J Bacteriol* **189**: 3591-3602.
1462 Gibson, K.E., Kobayashi, H., and Walker, G.C. (2008) Molecular determinants of a symbiotic chronic
1463 infection. *Annu Rev Genet* **42**: 413-441.

1464 Godessart, P., Lannoy, A., Dieu, M., Van der Verren, S.E., Soumillion, P., Collet, J.F., Remaut, H., Renard,
1465 P., and De Bolle, X. (2021) beta-Barrels covalently link peptidoglycan and the outer membrane in
1466 the alpha-proteobacterium *Brucella abortus*. *Nat Microbiol* **6**: 27-33.
1467 Graham, P.H., and Vance, C.P. (2003) Legumes: Importance and Constraints to Greater Use. *Plant*
1468 *Physiology* **131**: 872-877.
1469 Greenwich, J.L., Heckel, B.C., Alakavuklar, M.A., and Fuqua, C. (2023) The ChvG-ChvI Regulatory
1470 Network: A Conserved Global Regulatory Circuit Among the Alphaproteobacteria with Pervasive
1471 Impacts on Host Interactions and Diverse Cellular Processes. *Annu Rev Microbiol*.
1472 Griffitts, J.S., Carlyon, R.E., Erickson, J.H., Moulton, J.L., Barnett, M.J., Toman, C.J., and Long, S.R. (2008)
1473 A Sinorhizobium meliloti osmosensory two-component system required for cyclic glucan export
1474 and symbiosis. *Mol Microbiol* **69**: 479-490.
1475 Griffitts, J.S., and Long, S.R. (2008) A symbiotic mutant of *Sinorhizobium meliloti* reveals a novel genetic
1476 pathway involving succinoglycan biosynthetic functions. *Mol Microbiol* **67**: 1292-1306.
1477 Guzman-Verri, C., Manterola, L., Sola-Landa, A., Parra, A., Cloeckaert, A., Garin, J., Gorvel, J.P., Moriyon,
1478 I., Moreno, E., and Lopez-Goni, I. (2002) The two-component system BvrR/BvrS essential for
1479 *Brucella abortus* virulence regulates the expression of outer membrane proteins with
1480 counterparts in members of the Rhizobiaceae. *Proc Natl Acad Sci U S A* **99**: 12375-12380.
1481 Guzman, L.M., Belin, D., Carson, M.J., and Beckwith, J. (1995) Tight regulation, modulation, and high-
1482 level expression by vectors containing the arabinose PBAD promoter. *J Bacteriol* **177**: 4121-
1483 4130.
1484 Haag, A.F., Baloban, M., Sani, M., Kerscher, B., Pierre, O., Farkas, A., Longhi, R., Boncompagni, E.,
1485 Herouart, D., Dall'angelo, S., Kondorosi, E., Zanda, M., Mergaert, P., and Ferguson, G.P. (2011)
1486 Protection of *Sinorhizobium* against host cysteine-rich antimicrobial peptides is critical for
1487 symbiosis. *PLoS Biol* **9**: e1001169.
1488 Hawkins, J.P., Geddes, B.A., and Oresnik, I.J. (2017) Succinoglycan Production Contributes to Acidic pH
1489 Tolerance in *Sinorhizobium meliloti* Rm1021. *Mol Plant Microbe Interact* **30**: 1009-1019.
1490 Hawkins, J.P., and Oresnik, I.J. (2021) The Rhizobium-Legume Symbiosis: Co-opting Successful Stress
1491 Management. *Front Plant Sci* **12**: 796045.
1492 Heavner, M.E., Qiu, W.G., and Cheng, H.P. (2015) Phylogenetic Co-Occurrence of ExoR, ExoS, and ChvI,
1493 Components of the RSI Bacterial Invasion Switch, Suggests a Key Adaptive Mechanism
1494 Regulating the Transition between Free-Living and Host-Invading Phases in Rhizobiales. *PLoS*
1495 *One* **10**: e0135655.
1496 Heckel, B.C., Tomlinson, A.D., Morton, E.R., Choi, J.H., and Fuqua, C. (2014) *Agrobacterium tumefaciens*
1497 ExoR controls acid response genes and impacts exopolysaccharide synthesis, horizontal gene
1498 transfer, and virulence gene expression. *J Bacteriol* **196**: 3221-3233.
1499 Hellweg, C., Pühler, A., and Weidner, S. (2009) The time course of the transcriptomic response of
1500 *Sinorhizobium meliloti* 1021 following a shift to acidic pH. *BMC Microbiol* **9**: 37.
1501 Herridge, D.F., Peoples, M.B., and Boddey, R.M. (2008) Global inputs of biological nitrogen fixation in
1502 agricultural systems. *PLANT AND SOIL* **311**: 1-18.
1503 Hews, C.L., Cho, T., Rowley, G., and Raivio, T.L. (2019) Maintaining Integrity Under Stress: Envelope
1504 Stress Response Regulation of Pathogenesis in Gram-Negative Bacteria. *Front Cell Infect*
1505 *Microbiol* **9**: 313.
1506 Hoang, H.H., Gurich, N., and Gonzalez, J.E. (2008) Regulation of motility by the ExpR/Sin quorum-sensing
1507 system in *Sinorhizobium meliloti*. *J Bacteriol* **190**: 861-871.
1508 Horváth, B., Domonkos, A., Kereszt, A., Szucs, A., Abraham, E., Ayaydin, F., Boka, K., Chen, Y., Chen, R.,
1509 Murray, J.D., Udvardi, M.K., Kondorosi, E., and Kalo, P. (2015) Loss of the nodule-specific
1510 cysteine rich peptide, NCR169, abolishes symbiotic nitrogen fixation in the *Medicago truncatula*
1511 *dnf7* mutant. *Proc Natl Acad Sci U S A* **112**: 15232-15237.

House, B.L., Mortimer, M.W., and Kahn, M.L. (2004) New recombination methods for *Sinorhizobium meliloti* genetics. *Appl Environ Microbiol* **70**: 2806-2815.

Humphreys, S., Stevenson, A., Bacon, A., Weinhardt, A.B., and Roberts, M. (1999) The alternative sigma factor, sigmaE, is critically important for the virulence of *Salmonella typhimurium*. *Infect Immun* **67**: 1560-1568.

Isaac, D.D., Pinkner, J.S., Hultgren, S.J., and Silhavy, T.J. (2005) The extracytoplasmic adaptor protein CpxP is degraded with substrate by DegP. *Proc Natl Acad Sci U S A* **102**: 17775-17779.

Jones, K.M. (2012) Increased production of the exopolysaccharide succinoglycan enhances *Sinorhizobium meliloti* 1021 symbiosis with the host plant *Medicago truncatula*. *J Bacteriol* **194**: 4322-4331.

Jones, K.M., Kobayashi, H., Davies, B.W., Taga, M.E., and Walker, G.C. (2007) How rhizobial symbionts invade plants: the *Sinorhizobium-Medicago* model. *Nat Rev Microbiol* **5**: 619-633.

Jones, K.M., Sharopova, N., Lohar, D.P., Zhang, J.Q., VandenBosch, K.A., and Walker, G.C. (2008) Differential response of the plant *Medicago truncatula* to its symbiont *Sinorhizobium meliloti* or an exopolysaccharide-deficient mutant. *Proc Natl Acad Sci U S A* **105**: 704-709.

Juncker, A.S., Willenbrock, H., Von Heijne, G., Brunak, S., Nielsen, H., and Krogh, A. (2003) Prediction of lipoprotein signal peptides in Gram-negative bacteria. *Protein Sci* **12**: 1652-1662.

Kawaharada, Y., Kelly, S., Nielsen, M.W., Hjuler, C.T., Gysel, K., Muszynski, A., Carlson, R.W., Thygesen, M.B., Sandal, N., Asmussen, M.H., Vinther, M., Andersen, S.U., Krusell, L., Thirup, S., Jensen, K.J., Ronson, C.W., Blaise, M., Radutoiu, S., and Stougaard, J. (2015) Receptor-mediated exopolysaccharide perception controls bacterial infection. *Nature* **523**: 308-312.

Kawaharada, Y., Nielsen, M.W., Kelly, S., James, E.K., Andersen, K.R., Rasmussen, S.R., Fuchtbauer, W., Madsen, L.H., Heckmann, A.B., Radutoiu, S., and Stougaard, J. (2017) Differential regulation of the Epr3 receptor coordinates membrane-restricted rhizobial colonization of root nodule primordia. *Nat Commun* **8**: 14534.

Keating, D.H. (2007) The *Sinorhizobium meliloti* ExoR protein is required for the downregulation of *lpsS* transcription and succinoglycan biosynthesis in response to divalent cations. *FEMS Microbiol Lett* **267**: 23-29.

Kelly, S.J., Muszynski, A., Kawaharada, Y., Hubber, A.M., Sullivan, J.T., Sandal, N., Carlson, R.W., Stougaard, J., and Ronson, C.W. (2013) Conditional requirement for exopolysaccharide in the *Mesorhizobium-Lotus* symbiosis. *Mol Plant Microbe Interact* **26**: 319-329.

Khan, S.R., Gaines, J., Roop, R.M., 2nd, and Farrand, S.K. (2008) Broad-host-range expression vectors with tightly regulated promoters and their use to examine the influence of TraR and TraM expression on Ti plasmid quorum sensing. *Appl Environ Microbiol* **74**: 5053-5062.

Kim, M., Chen, Y., Xi, J., Waters, C., Chen, R., and Wang, D. (2015) An antimicrobial peptide essential for bacterial survival in the nitrogen-fixing symbiosis. *Proc Natl Acad Sci U S A* **112**: 15238-15243.

Kovacs-Simon, A., Titball, R.W., and Michell, S.L. (2011) Lipoproteins of bacterial pathogens. *Infect Immun* **79**: 548-561.

Krol, E., and Becker, A. (2004) Global transcriptional analysis of the phosphate starvation response in *Sinorhizobium meliloti* strains 1021 and 2011. *Mol Genet Genomics* **272**: 1-17.

Krol, E., Klaner, C., Gnau, P., Kaever, V., Essen, L.O., and Becker, A. (2016) Cyclic mononucleotide- and Clr-dependent gene regulation in *Sinorhizobium meliloti*. *Microbiology* **162**: 1840-1856.

Lai, K.K., Davis-Richardson, A.G., Dias, R., and Triplett, E.W. (2016) Identification of the Genes Required for the Culture of *Liberibacter crescens*, the Closest Cultured Relative of the *Liberibacter* Plant Pathogens. *Front Microbiol* **7**: 547.

Lakey, B.D., Myers, K.S., Alberge, F., Mettert, E.L., Kiley, P.J., Noguera, D.R., and Donohue, T.J. (2022) The essential *Rhodobacter sphaeroides* CenKR two-component system regulates cell division and envelope biosynthesis. *PLoS Genet* **18**: e1010270.

Lamontagne, J., Butler, H., Chaves-Olarte, E., Hunter, J., Schirm, M., Paquet, C., Tian, M., Kearney, P., Hamaidi, L., Chelsky, D., Moriyon, I., Moreno, E., and Paramithiotis, E. (2007) Extensive cell envelope modulation is associated with virulence in *Brucella abortus*. *J Proteome Res* **6**: 1519-1529.

Larrainzar, E., Gil-Quintana, E., Seminario, A., Arrese-Igor, C., and Gonzalez, E.M. (2014) Nodule carbohydrate catabolism is enhanced in the *Medicago truncatula* A17-*Sinorhizobium medicae* WSM419 symbiosis. *Front Microbiol* **5**: 447.

Ledermann, R., Schulte, C.C.M., and Poole, P.S. (2021) How Rhizobia Adapt to the Nodule Environment. *J Bacteriol* **203**: e0053920.

Lehman, A.P., and Long, S.R. (2013) Exopolysaccharides from *Sinorhizobium meliloti* can protect against H2O2-dependent damage. *J Bacteriol* **195**: 5362-5369.

LeVier, K., Phillips, R.W., Grippe, V.K., Roop, R.M., 2nd, and Walker, G.C. (2000) Similar requirements of a plant symbiont and a mammalian pathogen for prolonged intracellular survival. *Science* **287**: 2492-2493.

Li, L., Jia, Y., Hou, Q., Charles, T.C., Nester, E.W., and Pan, S.Q. (2002) A global pH sensor: *Agrobacterium* sensor protein ChvG regulates acid-inducible genes on its two chromosomes and Ti plasmid. *Proc Natl Acad Sci U S A* **99**: 12369-12374.

Li, S. (2018). *Role of a bacterial polar adhesion factor during legume-microbe symbiosis* [Master's thesis]. San Francisco State University, San Francisco, CA. http://hdl.handle.net/10211.3/199775

Long, S., Reed, J.W., Himawan, J., and Walker, G.C. (1988) Genetic analysis of a cluster of genes required for synthesis of the calcofluor-binding exopolysaccharide of *Rhizobium meliloti*. *J Bacteriol* **170**: 4239-4248.

Long, S.R. (2016) SnapShot: Signaling in Symbiosis. *Cell* **167**: 582-582 e581.

Lu, H.Y., and Cheng, H.P. (2010) Autoregulation of *Sinorhizobium meliloti exoR* gene expression. *Microbiology (Reading, England)* **156**: 2092-2101.

Lu, H.Y., Luo, L., Yang, M.H., and Cheng, H.P. (2012) *Sinorhizobium meliloti* ExoR is the target of periplasmic proteolysis. *J Bacteriol* **194**: 4029-4040.

Lund, J., Tedesco, P., Duke, K., Wang, J., Kim, S.K., and Johnson, T.E. (2002) Transcriptional profile of aging in *C. elegans*. *Curr Biol* **12**: 1566-1573.

Luo, L., Yao, S.Y., Becker, A., Rüberg, S., Yu, G.Q., Zhu, J.B., and Cheng, H.P. (2005) Two new *Sinorhizobium meliloti* LysR-type transcriptional regulators required for nodulation. *J Bacteriol* **187**: 4562-4572.

Maillet, F., Fournier, J., Mendis, H.C., Tadege, M., Wen, J., Ratet, P., Mysore, K.S., Gough, C., and Jones, K.M. (2020) *Sinorhizobium meliloti* succinylated high-molecular-weight succinoglycan and the *Medicago truncatula* LysM receptor-like kinase MtLYK10 participate independently in symbiotic infection. *Plant J* **102**: 311-326.

Manterola, L., Guzman-Verri, C., Chaves-Olarte, E., Barquero-Calvo, E., de Miguel, M.J., Moriyon, I., Grillo, M.J., Lopez-Goni, I., and Moreno, E. (2007) BvrR/BvrS-controlled outer membrane proteins Omp3a and Omp3b are not essential for *Brucella abortus* virulence. *Infect Immun* **75**: 4867-4874.

Manterola, L., Moriyon, I., Moreno, E., Sola-Landa, A., Weiss, D.S., Koch, M.H., Howe, J., Brandenburg, K., and Lopez-Goni, I. (2005) The lipopolysaccharide of *Brucella abortus* BvrS/BvrR mutants contains lipid A modifications and has higher affinity for bactericidal cationic peptides. *J Bacteriol* **187**: 5631-5639.

Mantis, N.J., and Winans, S.C. (1993) The chromosomal response regulatory gene *chvI* of *Agrobacterium tumefaciens* complements an *Escherichia coli phoB* mutation and is required for virulence. *J Bacteriol* **175**: 6626-6636.

1607 Maroti, G., Downie, J.A., and Kondorosi, E. (2015) Plant cysteine-rich peptides that inhibit pathogen
1608 growth and control rhizobial differentiation in legume nodules. *Curr Opin Plant Biol* **26**: 57-63.
1609 Martin, M.O., and Long, S.R. (1984) Generalized transduction in *Rhizobium meliloti*. *J Bacteriol* **159**: 125-
1610 129.
1611 Martinez-Nunez, C., Altamirano-Silva, P., Alvarado-Guillen, F., Moreno, E., Guzman-Verri, C., and Chaves-
1612 Olarte, E. (2010) The two-component system BvrR/BvrS regulates the expression of the type IV
1613 secretion system VirB in *Brucella abortus*. *J Bacteriol* **192**: 5603-5608.
1614 Masson-Boivin, C., and Sachs, J.L. (2018) Symbiotic nitrogen fixation by rhizobia-the roots of a success
1615 story. *Curr Opin Plant Biol* **44**: 7-15.
1616 Meade, H.M., Long, S.R., Ruvkun, G.B., Brown, S.E., and Ausubel, F.M. (1982) Physical and genetic
1617 characterization of symbiotic and auxotrophic mutants of *Rhizobium meliloti* induced by
1618 transposon Tn5 mutagenesis. *J Bacteriol* **149**: 114-122.
1619 Mendis, H.C., Madzima, T.F., Queiroux, C., and Jones, K.M. (2016) Function of Succinoglycan
1620 Polysaccharide in *Sinorhizobium meliloti* Host Plant Invasion Depends on Succinylation, Not
1621 Molecular Weight. *mBio* **7**.
1622 Mergaert, P., Nikovics, K., Kelemen, Z., Maunoury, N., Vaubert, D., Kondorosi, A., and Kondorosi, E.
1623 (2003) A novel family in *Medicago truncatula* consisting of more than 300 nodule-specific genes
1624 coding for small, secreted polypeptides with conserved cysteine motifs. *Plant Physiol* **132**: 161-
1625 173.
1626 Miller-Williams, M., Loewen, P.C., and Oresnik, I.J. (2006) Isolation of salt-sensitive mutants of
1627 *Sinorhizobium meliloti* strain Rm1021. *Microbiology (Reading, England)* **152**: 2049-2059.
1628 Mistry, J., Chuguransky, S., Williams, L., Qureshi, M., Salazar, G.A., Sonnhammer, E.L.L., Tosatto, S.C.E.,
1629 Paladin, L., Raj, S., Richardson, L.J., Finn, R.D., and Bateman, A. (2021) Pfam: The protein families
1630 database in 2021. *Nucleic Acids Res* **49**: D412-d419.
1631 Mitchell, A.M., and Silhavy, T.J. (2019) Envelope stress responses: balancing damage repair and toxicity.
1632 *Nat Rev Microbiol* **17**: 417-428.
1633 Morris, J., and Gonzalez, J.E. (2009) The novel genes *emmABC* are associated with exopolysaccharide
1634 production, motility, stress adaptation, and symbiosis in *Sinorhizobium meliloti*. *J Bacteriol* **191**:
1635 5890-5900.
1636 Mostafavi, M., Lewis, J.C., Saini, T., Bustamante, J.A., Gao, I.T., Tran, T.T., King, S.N., Huang, Z., and Chen,
1637 J.C. (2014) Analysis of a taurine-dependent promoter in *Sinorhizobium meliloti* that offers tight
1638 modulation of gene expression. *BMC Microbiol* **14**: 295.
1639 Motulsky, H.J., "Interpreting results: Mann-Whitney test", GraphPad Statistics Guide. Accessed April 20,
1640 2023. https://www.graphpad.com/guides/prism/latest/statistics/how_the_mann-
1641 whitney_test_works.htm
1642 Nicoloff, H., Gopalkrishnan, S., and Ades, S.E. (2017) Appropriate Regulation of the σ(E)-Dependent
1643 Envelope Stress Response Is Necessary To Maintain Cell Envelope Integrity and Stationary-Phase
1644 Survival in *Escherichia coli*. *J Bacteriol* **199**.
1645 Oke, V., and Long, S.R. (1999) Bacterial genes induced within the nodule during the Rhizobium-legume
1646 symbiosis. *Mol Microbiol* **32**: 837-849.
1647 Olivares, J., Bedmar, E.J., and Sanjuán, J. (2013) Biological nitrogen fixation in the context of global
1648 change. *Mol Plant Microbe Interact* **26**: 486-494.
1649 Ozga, D.A., Lara, J.C., and Leig, J.A. (1994) The regulation of exopolysaccharide production is important
1650 at two levels of nodule development in *Rhizobium meliloti*. *Mol Plant Microbe Interact* **7**: 758-
1651 765.
1652 Pagliai, F.A., Gardner, C.L., Bojilova, L., Sarnegrim, A., Tamayo, C., Potts, A.H., Teplitski, M., Folimonova,
1653 S.Y., Gonzalez, C.F., and Lorca, G.L. (2014) The transcriptional activator LdtR from 'Candidatus
1654 *Liberibacter asiaticus*' mediates osmotic stress tolerance. *PLoS Pathog* **10**: e1004101.

Pellock, B.J., Cheng, H.P., and Walker, G.C. (2000) Alfalfa root nodule invasion efficiency is dependent on *Sinorhizobium meliloti* polysaccharides. *J Bacteriol* **182**: 4310-4318.

Penterman, J., Abo, R.P., De Nisco, N.J., Arnold, M.F., Longhi, R., Zanda, M., and Walker, G.C. (2014) Host plant peptides elicit a transcriptional response to control the *Sinorhizobium meliloti* cell cycle during symbiosis. *Proceedings of the National Academy of Sciences of the United States of America* **111**: 3561-3566.

Perry, B.J., Akter, M.S., and Yost, C.K. (2016) The Use of Transposon Insertion Sequencing to Interrogate the Core Functional Genome of the Legume Symbiont *Rhizobium leguminosarum*. *Front Microbiol* **7**: 1873.

Poole, P., Ramachandran, V., and Terpolilli, J. (2018) Rhizobia: from saprophytes to endosymbionts. *Nat Rev Microbiol* **16**: 291-303.

Price, M.N., Wetmore, K.M., Waters, R.J., Callaghan, M., Ray, J., Liu, H., Kuehl, J.V., Melnyk, R.A., Lamson, J.S., Suh, Y., Carlson, H.K., Esquivel, Z., Sadeeshkumar, H., Chakraborty, R., Zane, G.M., Rubin, B.E., Wall, J.D., Visel, A., Bristow, J., Blow, M.J., Arkin, A.P., and Deutschbauer, A.M. (2018) Mutant phenotypes for thousands of bacterial genes of unknown function. *Nature* **557**: 503-509.

Price, P.A., Tanner, H.R., Dillon, B.A., Shabab, M., Walker, G.C., and Griffitts, J.S. (2015) Rhizobial peptidase HrrP cleaves host-encoded signaling peptides and mediates symbiotic compatibility. *Proc Natl Acad Sci U S A* **112**: 15244-15249.

Quandt, J., and Hynes, M.F. (1993) Versatile suicide vectors which allow direct selection for gene replacement in gram-negative bacteria. *Gene* **127**: 15-21.

Quebatte, M., Dehio, M., Tropel, D., Basler, A., Toller, I., Raddatz, G., Engel, P., Huser, S., Schein, H., Lindroos, H.L., Andersson, S.G., and Dehio, C. (2010) The BatR/BatS two-component regulatory system controls the adaptive response of *Bartonella henselae* during human endothelial cell infection. *J Bacteriol* **192**: 3352-3367.

Quintero-Yanes, A., Mayard, A., and Hallez, R. (2022) The two-component system ChvGI maintains cell envelope homeostasis in *Caulobacter crescentus*. *PLoS Genet* **18**: e1010465.

Raivio, T.L. (2005) Envelope stress responses and Gram-negative bacterial pathogenesis. *Mol Microbiol* **56**: 1119-1128.

Ratib, N.R., Sabio, E.Y., Mendoza, C., Barnett, M.J., Clover, S.B., Ortega, J.A., Dela Cruz, F.M., Balderas, D., White, H., Long, S.R., and Chen, E.J. (2018) Genome-wide identification of genes directly regulated by ChvI and a consensus sequence for ChvI binding in *Sinorhizobium meliloti*. *Mol Microbiol* **110**: 596-615.

Reeve, W., Chain, P., O'Hara, G., Ardley, J., Nandesena, K., Brau, L., Tiwari, R., Malfatti, S., Kiss, H., Lapidus, A., Copeland, A., Nolan, M., Land, M., Hauser, L., Chang, Y.J., Ivanova, N., Mavromatis, K., Markowitz, V., Kyrpides, N., Gollagher, M., Yates, R., Dilworth, M., and Howieson, J. (2010) Complete genome sequence of the *Medicago* microsymbiont *Ensifer* (*Sinorhizobium*) *medicae* strain WSM419. *Stand Genomic Sci* **2**: 77-86.

Reuber, T.L., and Walker, G.C. (1993) Biosynthesis of succinoglycan, a symbiotically important exopolysaccharide of Rhizobium meliloti. *Cell* **74**: 269-280.

Rivas-Solano, O., Van der Henst, M., Castillo-Zeledon, A., Suarez-Esquivel, M., Munoz-Vargas, L., Capitan-Barrios, Z., Thomson, N.R., Chaves-Olarte, E., Moreno, E., De Bolle, X., and Guzman-Verri, C. (2022) The regulon of *Brucella abortus* two-component system BvrR/BvrS reveals the coordination of metabolic pathways required for intracellular life. *PLoS One* **17**: e0274397.

Ryoji, M., Hsia, K., and Kaji, A. (1983) Read-through translation. *Trends in Biochemical Sciences* **8**: 88-90.

Sambrook, J., Fritsch, E.F., and Maniatis, T., (1989) *Molecular cloning: a laboratory manual*. Cold Spring Harbor Laboratory Press, Cold Spring Harbor, N.Y.

1702 Sankari, S., Babu, V.M.P., Bian, K., Alhhazmi, A., Andorfer, M.C., Avalos, D.M., Smith, T.A., Yoon, K.,
1703 Drennan, C.L., Yaffe, M.B., Lourido, S., and Walker, G.C. (2022) A haem-sequestering plant
1704 peptide promotes iron uptake in symbiotic bacteria. *Nat Microbiol* **7**: 1453-1465.
1705 Santos, M.R., Cosme, A.M., Becker, J.D., Medeiros, J.M., Mata, M.F., and Moreira, L.M. (2010) Absence
1706 of functional TolC protein causes increased stress response gene expression in *Sinorhizobium*
1707 *meliloti*. *BMC Microbiol* **10**: 180.
1708 Santos, M.R., Marques, A.T., Becker, J.D., and Moreira, L.M. (2014) The *Sinorhizobium meliloti* EmrR
1709 regulator is required for efficient colonization of *Medicago sativa* root nodules. *Mol Plant*
1710 *Microbe Interact* **27**: 388-399.
1711 Sayers, E.W., Bolton, E.E., Brister, J.R., Canese, K., Chan, J., Comeau, D.C., Connor, R., Funk, K., Kelly, C.,
1712 Kim, S., Madej, T., Marchler-Bauer, A., Lanczycki, C., Lathrop, S., Lu, Z., Thibaud-Nissen, F.,
1713 Murphy, T., Phan, L., Skripchenko, Y., Tse, T., Wang, J., Williams, R., Trawick, B.W., Pruitt, K.D.,
1714 and Sherry, S.T. (2022) Database resources of the national center for biotechnology information.
1715 *Nucleic Acids Res* **50**: D20-D26.
1716 Scharf, B., and Schmitt, R. (2002) Sensory transduction to the flagellar motor of *Sinorhizobium meliloti*. *J*
1717 *Mol Microbiol Biotechnol* **4**: 183-186.
1718 Sheehan, L.M., Budnick, J.A., Blanchard, C., Dunman, P.M., and Caswell, C.C. (2015) A LysR-family
1719 transcriptional regulator required for virulence in *Brucella abortus* is highly conserved among
1720 the alpha-proteobacteria. *Mol Microbiol* **98**: 318-328.
1721 Sola-Landa, A., Pizarro-Cerdá, J., Grilló, M.J., Moreno, E., Moriyón, I., Blasco, J.M., Gorvel, J.P., and
1722 López-Goñi, I. (1998) A two-component regulatory system playing a critical role in plant
1723 pathogens and endosymbionts is present in *Brucella abortus* and controls cell invasion and
1724 virulence. *Mol Microbiol* **29**: 125-138.
1725 Stanley, J., and Cervantes, E. (1991) Biology and genetics of the broad host range *Rhizobium* sp. NGR234.
1726 *Journal of Applied Bacteriology* **70**: 9-19.
1727 Stein, B.J., Fiebig, A., and Crosson, S. (2021) The ChvG-ChvI and NtrY-NtrX Two-Component Systems
1728 Coordinately Regulate Growth of *Caulobacter crescentus*. *J Bacteriol* **203**: e0019921.
1729 Sun, J., Rutherford, S.T., Silhavy, T.J., and Huang, K.C. (2022) Physical properties of the bacterial outer
1730 membrane. *Nat Rev Microbiol* **20**: 236-248.
1731 Swanson, J.A., Mulligan, J.T., and Long, S.R. (1993) Regulation of syrM and nodD3 in Rhizobium meliloti.
1732 *Genetics* **134**: 435-444.
1733 Tang, G., Li, Q., Xing, S., Li, N., Tang, Z., Yu, L., Yan, J., Li, X., and Luo, L. (2018) The LsrB Protein Is
1734 Required for *Agrobacterium tumefaciens* Interaction with Host Plants. *Mol Plant Microbe*
1735 *Interact* **31**: 951-961.
1736 Tata, M., Kumar, S., Lach, S.R., Saha, S., Hart, E.M., and Konovalova, A. (2021) High-throughput
1737 suppressor screen demonstrates that RcsF monitors outer membrane integrity and not Bam
1738 complex function. *Proc Natl Acad Sci U S A* **118**.
1739 Taylor, D.L., Bina, X.R., Slamti, L., Waldor, M.K., and Bina, J.E. (2014) Reciprocal regulation of resistance-
1740 nodulation-division efflux systems and the Cpx two-component system in *Vibrio cholerae*. *Infect*
1741 *Immun* **82**: 2980-2991.
1742 Terpolilli, J.J., O'Hara, G.W., Tiwari, R.P., Dilworth, M.J., and Howieson, J.G. (2008) The model legume
1743 *Medicago truncatula* A17 is poorly matched for N2 fixation with the sequenced microsymbiont
1744 *Sinorhizobium meliloti* 1021. *New Phytol* **179**: 62-66.
1745 Testerman, T.L., Vazquez-Torres, A., Xu, Y., Jones-Carson, J., Libby, S.J., and Fang, F.C. (2002) The
1746 alternative sigma factor sigmaE controls antioxidant defences required for *Salmonella* virulence
1747 and stationary-phase survival. *Mol Microbiol* **43**: 771-782.

1748 Tomlinson, A.D., Ramey-Hartung, B., Day, T.W., Merritt, P.M., and Fuqua, C. (2010) *Agrobacterium*
1749 *tumefaciens* ExoR represses succinoglycan biosynthesis and is required for biofilm formation and
1750 motility. *Microbiology (Reading, England)* **156**: 2670-2681.
1751 Trinick, M.J. (1980) Relationships Amongst the Fast-growing Rhizobia of *Lablab purpureus*, *Leucaena*
1752 *leucocephala*, *Mimosa* spp., *Acacia farnesiana* and *Sesbania grandiflora* and their Affinities with
1753 Other Rhizobial Groups. *Journal of Applied Bacteriology* **49**: 39-53.
1754 Van de Velde, W., Zehirov, G., Szatmari, A., Debreczeny, M., Ishihara, H., Kevei, Z., Farkas, A., Mikulass,
1755 K., Nagy, A., Tiricz, H., Satiat-Jeunemaitre, B., Alunni, B., Bourge, M., Kucho, K., Abe, M., Kereszt,
1756 A., Maroti, G., Uchiumi, T., Kondorosi, E., and Mergaert, P. (2010) Plant peptides govern terminal
1757 differentiation of bacteria in symbiosis. *Science* **327**: 1122-1126.
1758 Van Valen, L. (1973) A new evolutionary law. *Evol. Theory* **1**: 1-30.
1759 Vanderlinde, E.M., and Yost, C.K. (2012) Mutation of the sensor kinase *chvG* in *Rhizobium*
1760 *leguminosarum* negatively impacts cellular metabolism, outer membrane stability, and
1761 symbiosis. *J Bacteriol* **194**: 768-777.
1762 VanYperen, R.D., Orton, T.S., and Griffitts, J.S. (2015) Genetic analysis of signal integration by the
1763 *Sinorhizobium meliloti* sensor kinase FeuQ. *Microbiology (Reading, England)* **161**: 244-253.
1764 Viadas, C., Rodriguez, M.C., Sangari, F.J., Gorvel, J.P., Garcia-Lobo, J.M., and Lopez-Goni, I. (2010)
1765 Transcriptome analysis of the *Brucella abortus* BvrR/BvrS two-component regulatory system.
1766 *PLoS One* **5**: e10216.
1767 Vriezen, J.A., de Bruijn, F.J., and Nusslein, K. (2007) Responses of rhizobia to desiccation in relation to
1768 osmotic stress, oxygen, and temperature. *Appl Environ Microbiol* **73**: 3451-3459.
1769 Walsh, N.P., Alba, B.M., Bose, B., Gross, C.A., and Sauer, R.T. (2003) OMP peptide signals initiate the
1770 envelope-stress response by activating DegS protease via relief of inhibition mediated by its PDZ
1771 domain. *Cell* **113**: 61-71.
1772 Wang, C., Kemp, J., Da Fonseca, I.O., Equi, R.C., Sheng, X., Charles, T.C., and Sobral, B.W. (2010a)
1773 *Sinorhizobium meliloti* 1021 loss-of-function deletion mutation in *chvI* and its phenotypic
1774 characteristics. *Mol Plant Microbe Interact* **23**: 153-160.
1775 Wang, D., Griffitts, J., Starker, C., Fedorova, E., Limpens, E., Ivanov, S., Bisseling, T., and Long, S. (2010b)
1776 A nodule-specific protein secretory pathway required for nitrogen-fixing symbiosis. *Science* **327**:
1777 1126-1129.
1778 Wang, D., Xue, H., Wang, Y., Yin, R., Xie, F., and Luo, L. (2013) The *Sinorhizobium meliloti ntrX* gene is
1779 involved in succinoglycan production, motility, and symbiotic nodulation on alfalfa. *Appl Environ*
1780 *Microbiol* **79**: 7150-7159.
1781 Weiss, D.S., Chen, J.C., Ghigo, J.M., Boyd, D., and Beckwith, J. (1999) Localization of FtsI (PBP3) to the
1782 septal ring requires its membrane anchor, the Z ring, FtsA, FtsQ, and FtsL. *J Bacteriol* **181**: 508-
1783 520.
1784 Wells, D.H., Chen, E.J., Fisher, R.F., and Long, S.R. (2007) ExoR is genetically coupled to the ExoS-ChvI
1785 two-component system and located in the periplasm of *Sinorhizobium meliloti*. *Mol Microbiol*
1786 **64**: 647-664.
1787 Wiech, E.M., Cheng, H.P., and Singh, S.M. (2015) Molecular modeling and computational analyses
1788 suggests that the *Sinorhizobium meliloti* periplasmic regulator protein ExoR adopts a
1789 superhelical fold and is controlled by a unique mechanism of proteolysis. *Protein Sci* **24**: 319-
1790 327.
1791 Williams, M.A., Bouchier, J.M., Mason, A.K., and Brown, P.J.B. (2022) Activation of ChvG-ChvI regulon by
1792 cell wall stress confers resistance to beta-lactam antibiotics and initiates surface spreading in
1793 *Agrobacterium tumefaciens*. *PLoS Genet* **18**: e1010274.
1794 Wu, C.F., Lin, J.S., Shaw, G.C., and Lai, E.M. (2012) Acid-induced type VI secretion system is regulated by
1795 ExoR-ChvG/ChvI signaling cascade in *Agrobacterium tumefaciens*. *PLoS Pathog* **8**: e1002938.

1796 Xing, S., Zheng, W., An, F., Huang, L., Yang, X., Zeng, S., Li, N., Ouenzar, K., Yu, L., and Luo, L. (2022)
1797 Transcription Regulation of Cell Cycle Regulatory Genes Mediated by NtrX to Affect
1798 *Sinorhizobium meliloti* Cell Division. *Genes (Basel)* **13**.
1799 Yao, S.Y., Luo, L., Har, K.J., Becker, A., Rüberg, S., Yu, G.Q., Zhu, J.B., and Cheng, H.P. (2004)
1800 *Sinorhizobium meliloti* ExoR and ExoS proteins regulate both succinoglycan and flagellum
1801 production. *J Bacteriol* **186**: 6042-6049.
1802 Yuan, Z.C., Liu, P., Saenkham, P., Kerr, K., and Nester, E.W. (2008) Transcriptome profiling and functional
1803 analysis of *Agrobacterium tumefaciens* reveals a general conserved response to acidic conditions
1804 (pH 5.5) and a complex acid-mediated signaling involved in *Agrobacterium*-plant interactions. *J*
1805 *Bacteriol* **190**: 494-507.
1806

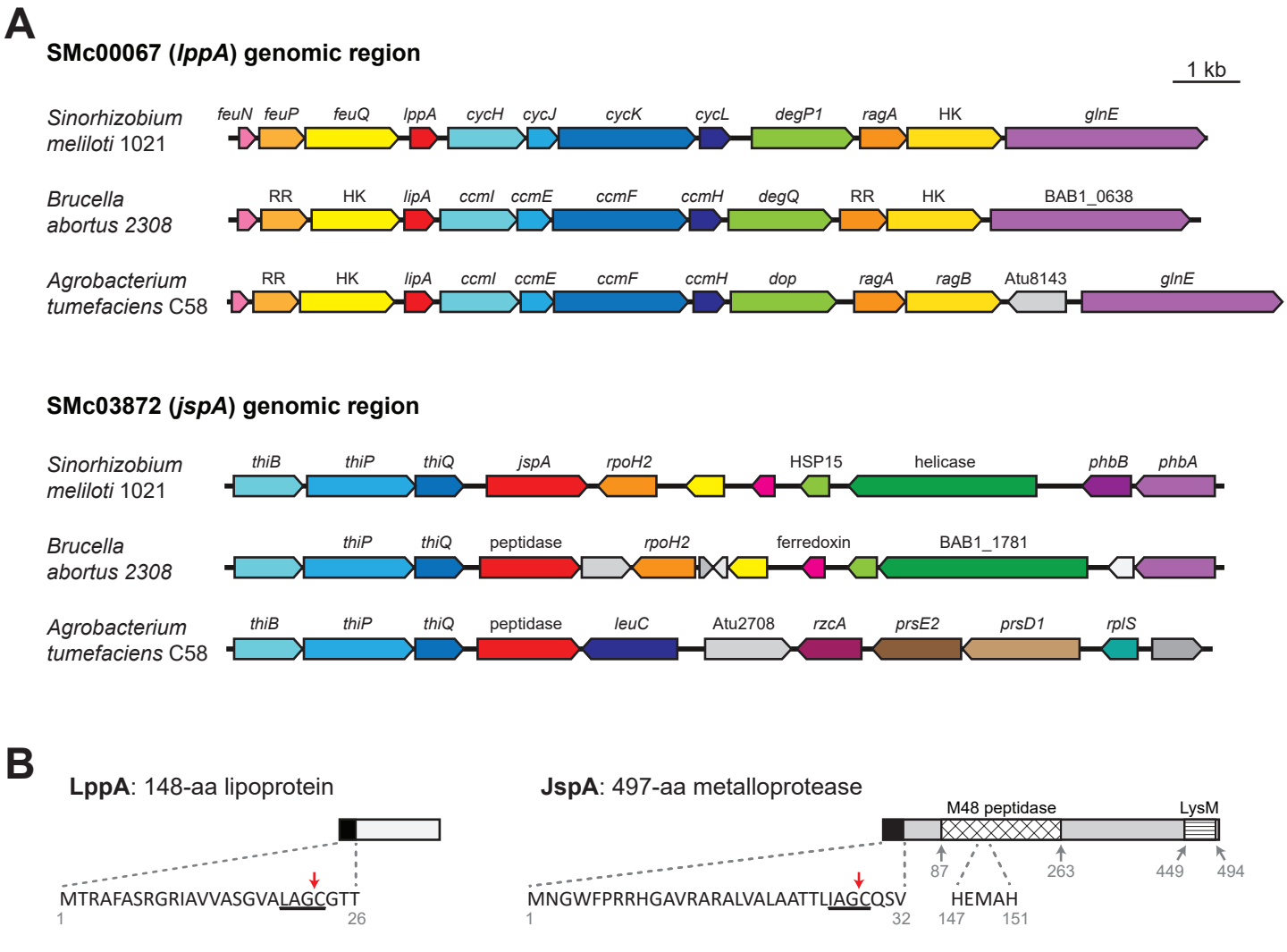

FIG. 1

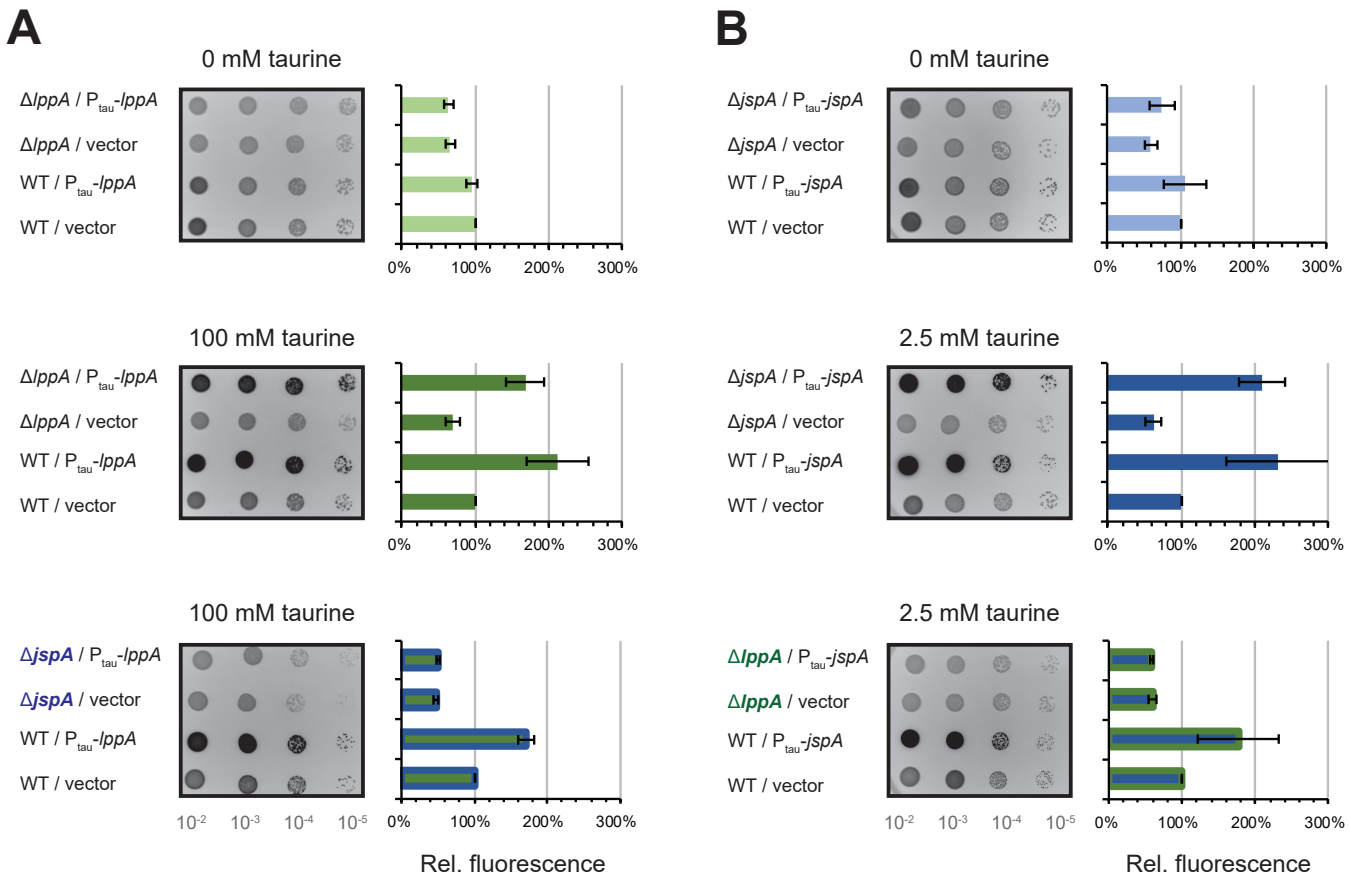

FIG. 2

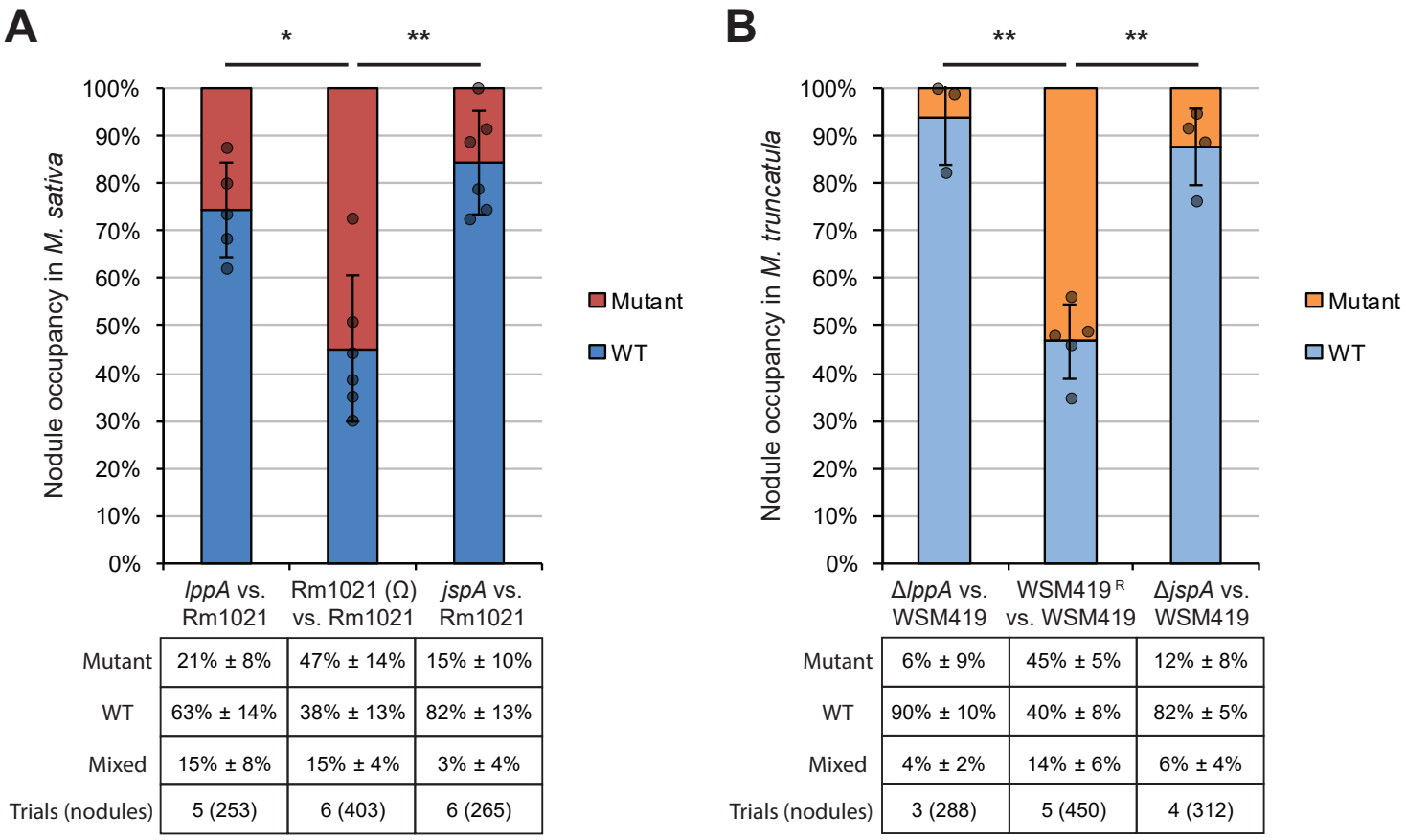

	lppA vs. Rm1021	Rm1021 (Ω) vs. Rm1021	*jspA* vs. Rm1021
Mutant	21% ± 8%	47% ± 14%	15% ± 10%
WT	63% ± 14%	38% ± 13%	82% ± 13%
Mixed	15% ± 8%	15% ± 4%	3% ± 4%
Trials (nodules)	5 (253)	6 (403)	6 (265)

	Δ*lppA* vs. WSM419	WSM419^{R} vs. WSM419	Δ*jspA* vs. WSM419
Mutant	6% ± 9%	45% ± 5%	12% ± 8%
WT	90% ± 10%	40% ± 8%	82% ± 5%
Mixed	4% ± 2%	14% ± 6%	6% ± 4%
Trials (nodules)	3 (288)	5 (450)	4 (312)

FIG. 3

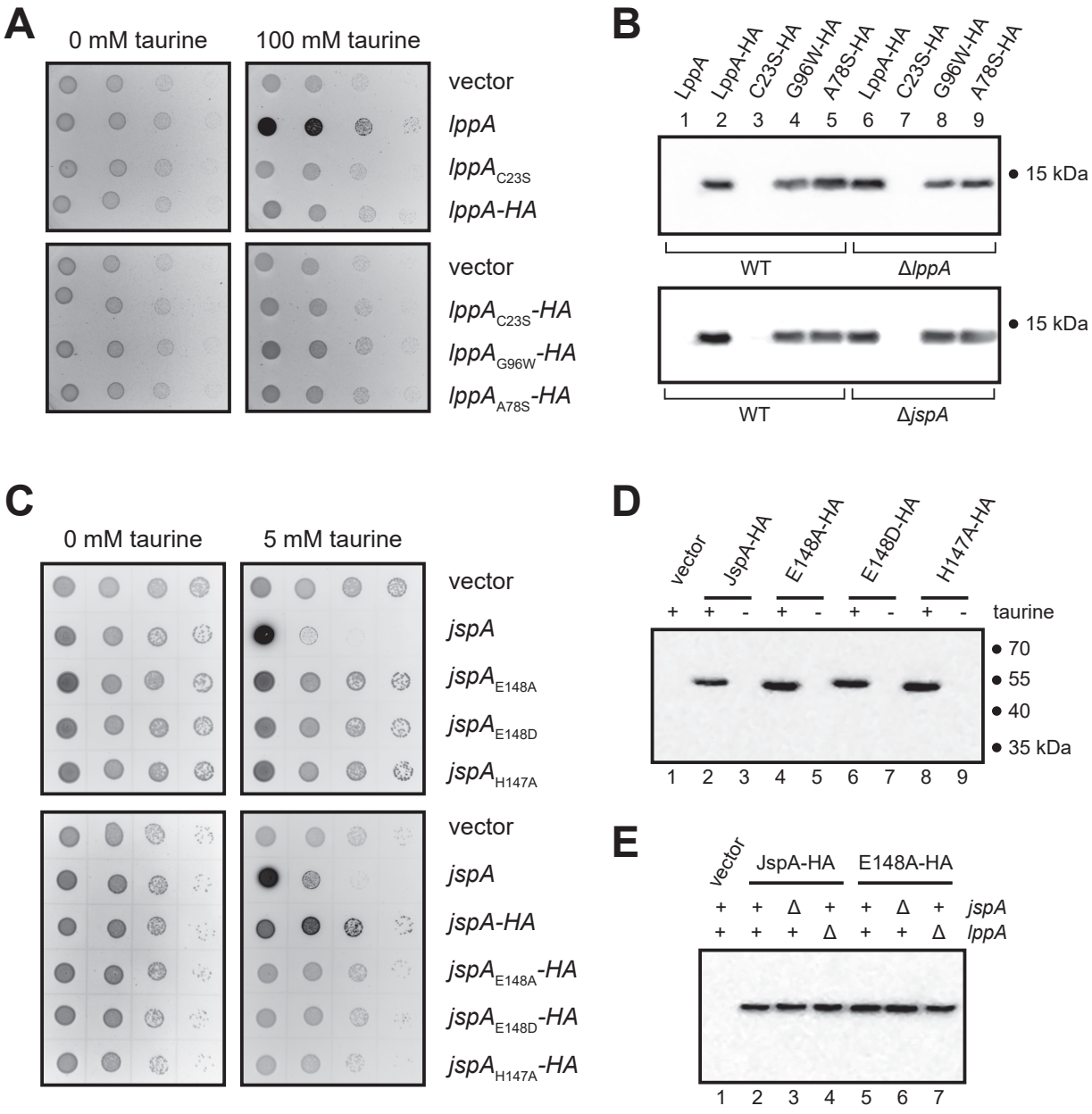

FIG. 4

A **Altered gene expression when JspA overexpressed > 1.5-fold change**

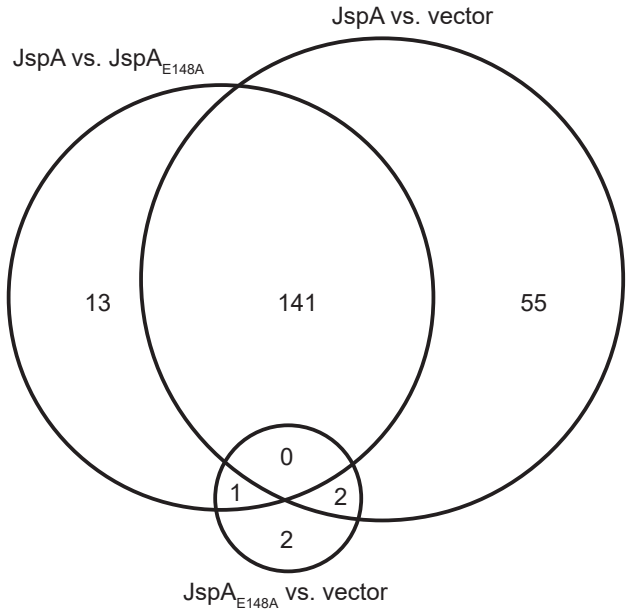

80 genes UP-regulated

Exopolysaccharide biosynthesis:	23
Regulators (including ChvI):	6
Metabolism:	6
Miscellaneous:	10
Hypothetical proteins:	35

61 genes DOWN-regulated

Flagellar biosynthesis and motility:	40
Pili biogenesis:	2
Metabolism and biosynthesis:	9
Regulators:	3
Miscellaneous:	1
Hypothetical proteins:	6

B **Comparisons of JspA and ExoR/ExoS transcriptomes and ChvI regulon**

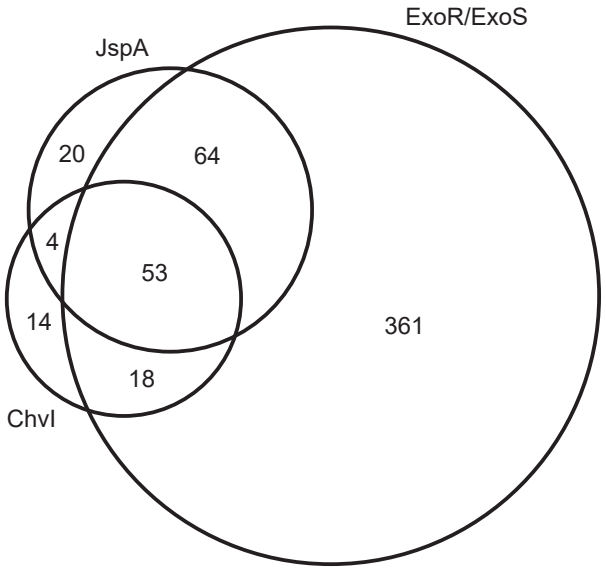

C **Comparisons of JspA and RpoH1 transcriptomes**

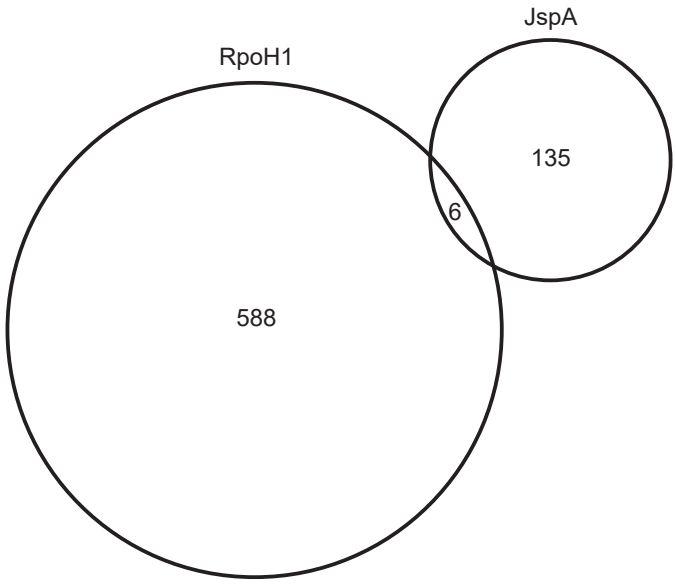

FIG. 5

A

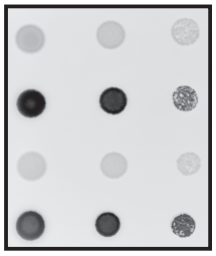

Rm1021	100%
exoS96::Tn5	380% ± 49%
Δ*lppA*	74% ± 5%
Δ*lppA exoS96::Tn5*	371% ± 45%
Rm1021	100%
exoS96::Tn5	404% ± 33%
Δ*jspA*	67% ± 3%
Δ*jspA exoS96::Tn5*	409% ± 12%

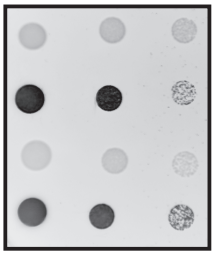

Rm1021	100%
exoR95::Tn5	363% ± 20%
Δ*lppA*	75% ± 1%
Δ*lppA exoR95::Tn5*	306% ± 65%
Rm1021	100%
exoR95::Tn5	365% ± 37%
Δ*jspA*	59% ± 15%
Δ*jspA exoR95::Tn5*	347% ± 63%

10^{-2} 10^{-3} 10^{-4} 10^{-2} 10^{-3} 10^{-4}

B

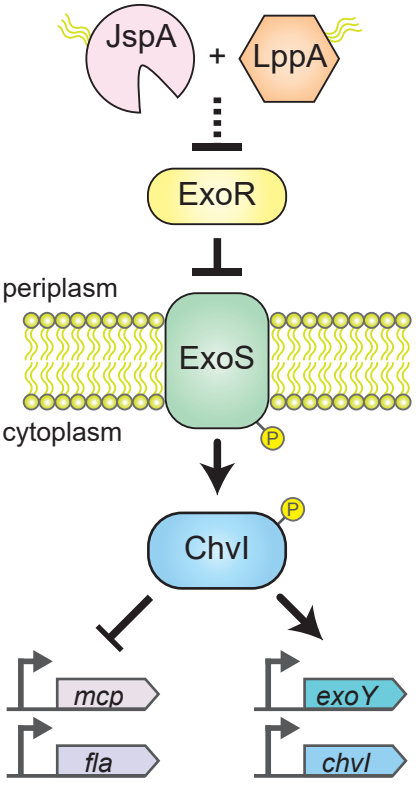

C

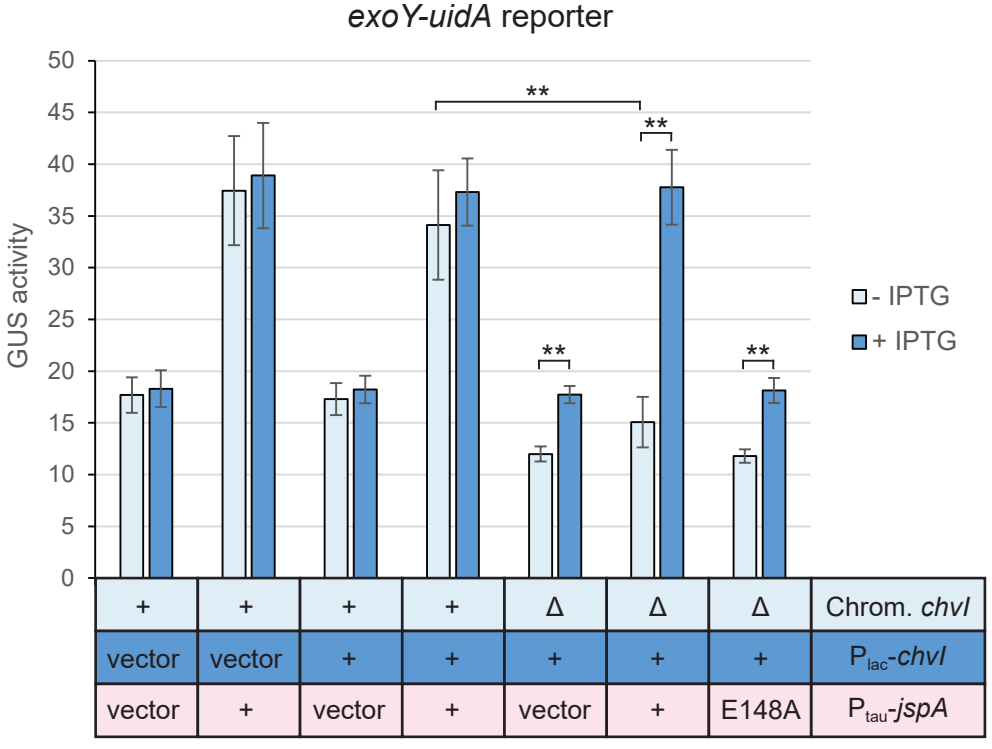

+	+	+	+	Δ	Δ	Δ	Chrom. *chvI*
vector	vector	+	+	+	+	+	P_{lac}-*chvI*
vector	+	vector	+	vector	+	E148A	P_{tau}-*jspA*

FIG. 6

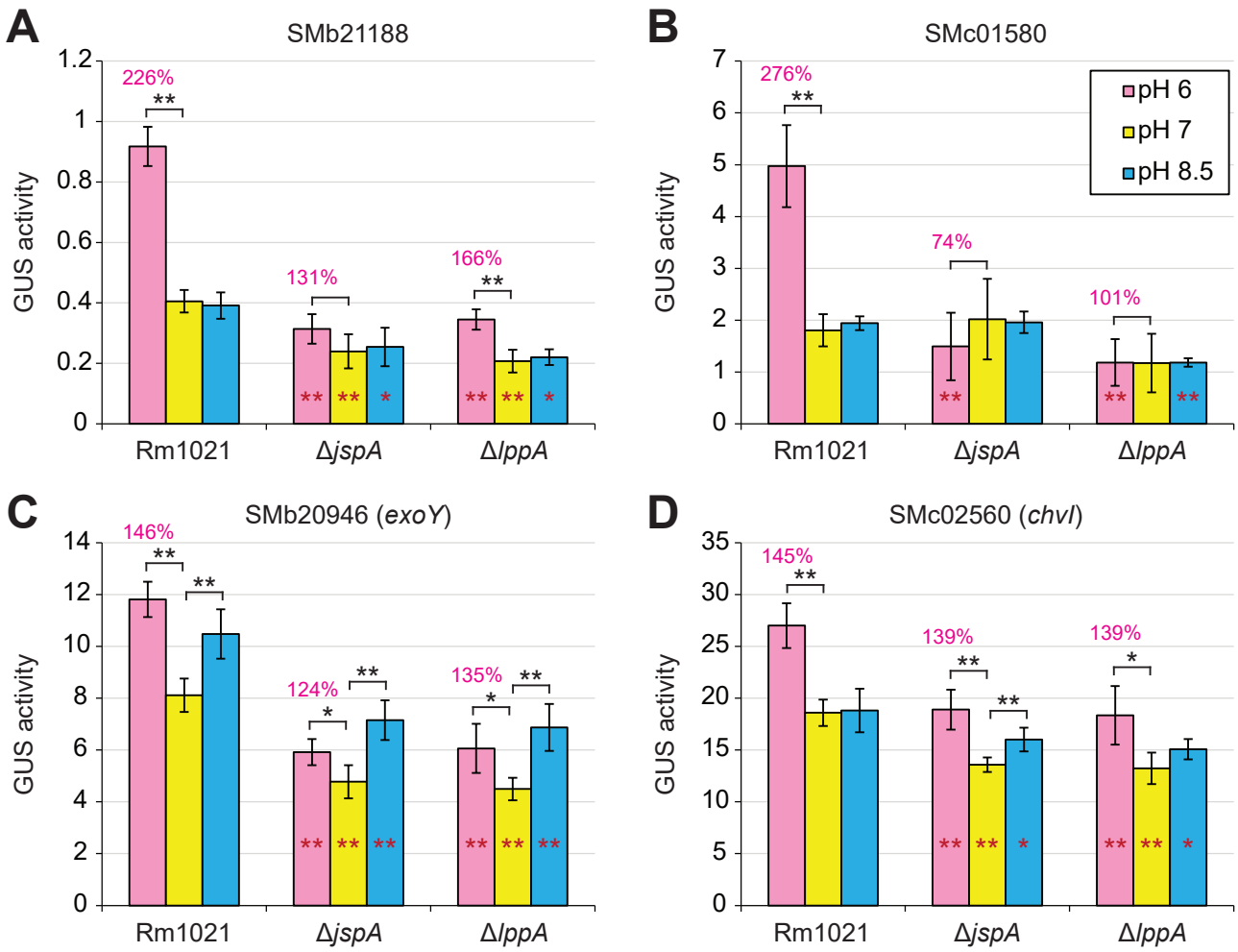

FIG. 7

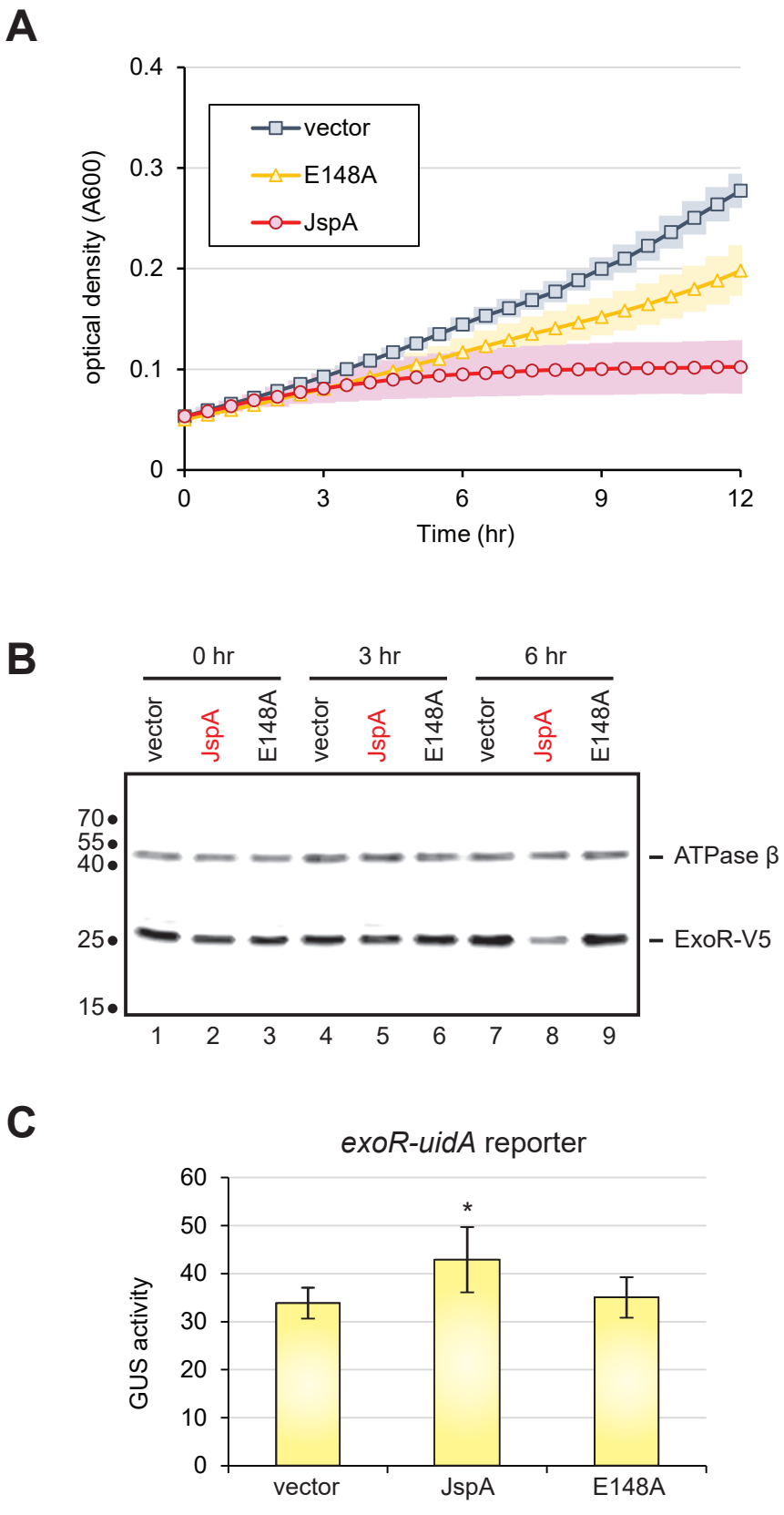

FIG. 8

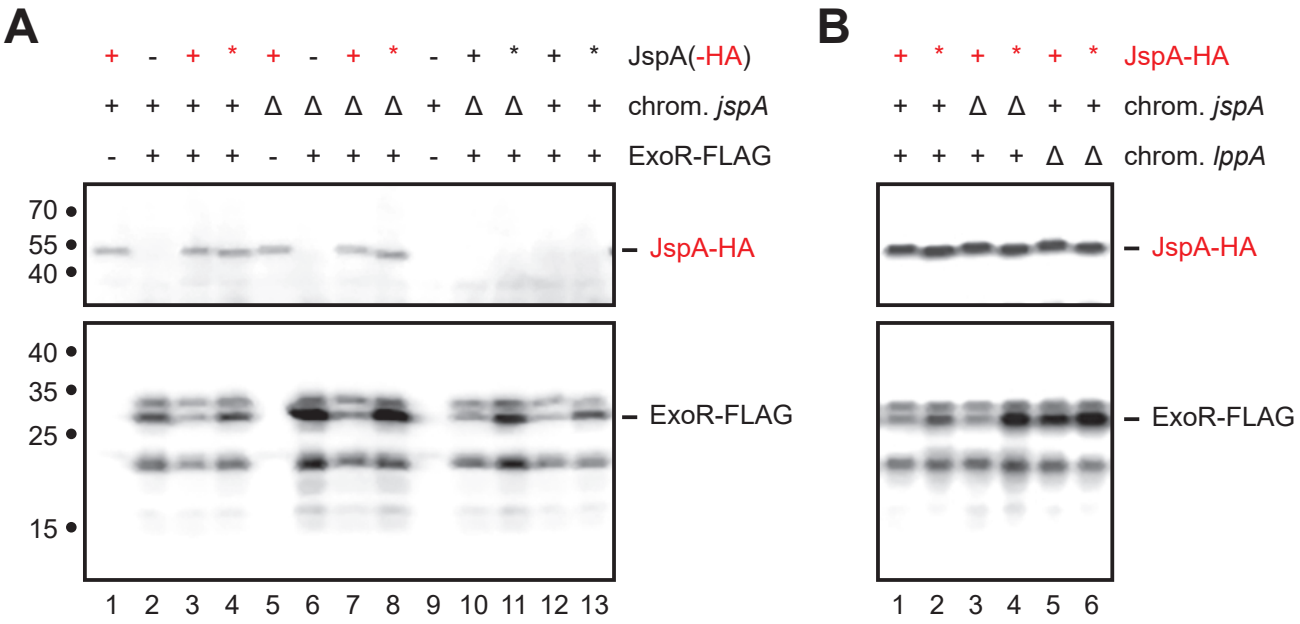

FIG. 9

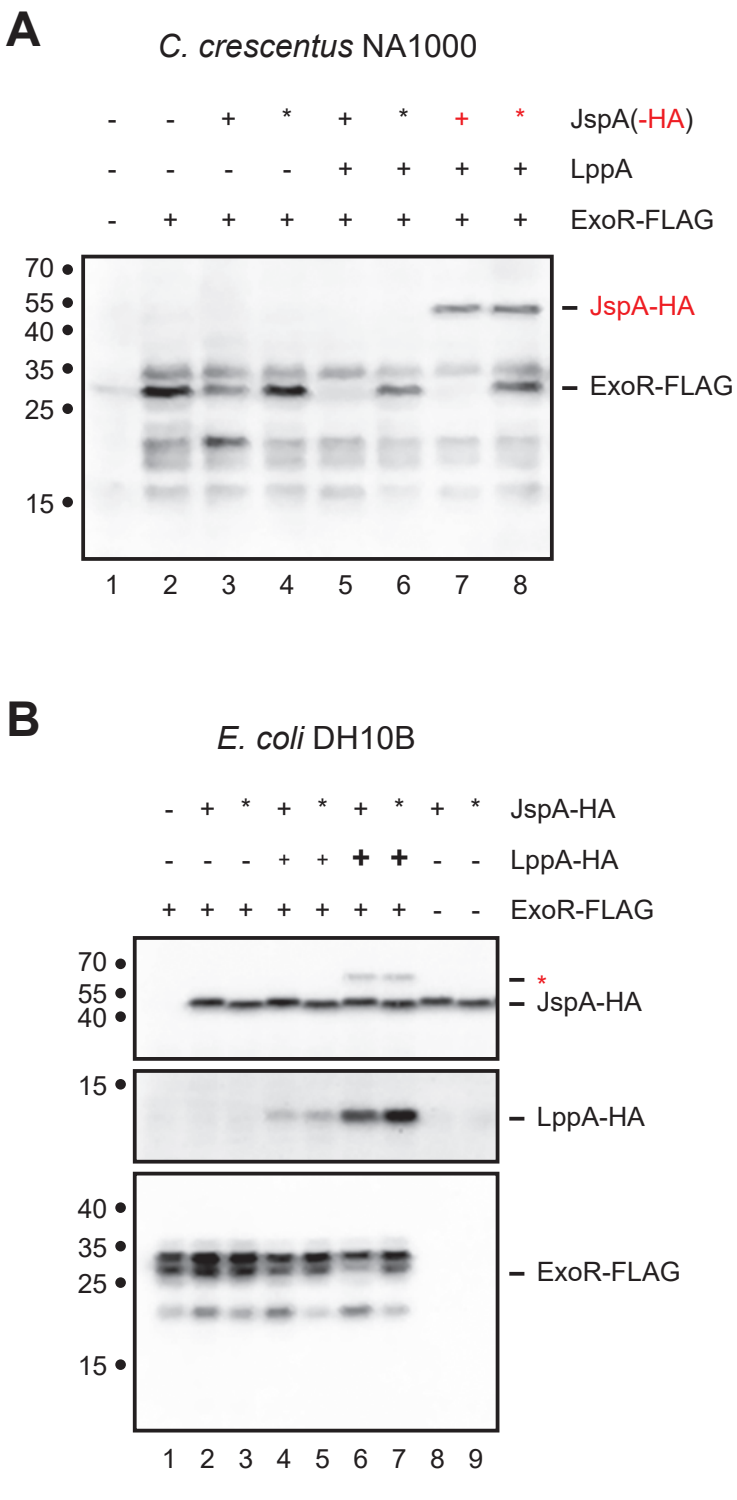

FIG. 10